frontiers | Frontiers in Earth Science

TYPE Original Research
PUBLISHED 02 February 2023
DOI 10.3389/feart.2023.1097101

OPEN ACCESS

EDITED BY
Wei Ju,
China University of Mining and Technology, China

REVIEWED BY
Yuan Neng,
China University of Petroleum Beijing, China
Guangyou Zhu,
Research Institute of Petroleum Exploration and Development (RIPED), China

*CORRESPONDENCE
Jinkai Xia,
1901110591@pku.edu.cn

SPECIALTY SECTION
This article was submitted to Structural Geology and Tectonics, a section of the journal Frontiers in Earth Science

RECEIVED 13 November 2022
ACCEPTED 18 January 2023
PUBLISHED 02 February 2023

CITATION
Xia J, Zhong Z, Huang S, Luo C, Lou H, Chang H, Li X and Wei L (2023), The proto-type basin and tectono-paleogeographic evolution of the Tarim basin in the Late Paleozoic.
Front. Earth Sci. 11:1097101.
doi: 10.3389/feart.2023.1097101

The proto-type basin and tectono-paleogeographic evolution of the Tarim basin in the Late Paleozoic

Jinkai Xia[1]*, Ziqi Zhong[1], Shaoying Huang[2], Caiming Luo[2], Hong Lou[2], Haining Chang[1], Xiang Li[1] and Lunyan Wei[1]

[1]The Key Laboratory of Orogenic Belts and Crustal Evolution, Ministry of Education, School of Earth and Space Sciences, Peking University, Beijing, China, [2]Institute of Petroleum Exploration and Development, Tarim Oilfield Company, Korla, China

The Tarim basin is a large composite and superimposed sedimentary basin that has undergone complex multi-period and polycyclic tectonic movements. Understanding the proto-type basin and tectono-paleogeographic evolution of this complex superimposed basin is important for understanding the basin-mountain coupling and dynamical mechanisms of the Paleo-Asian and Tethys tectonic systems as well as hydrocarbon exploration and development. Based on previous works, together with the recent exploration, and geological evidences, three global plate tectonic pattern maps, four Tarim proto-type basin maps (in present-day geographic coordinates) and four regional tectono-paleogeography maps (in paleogeographic coordinates) during the Late Paleozoic are provided in this paper. Based on these maps, the proto-type basin and tectono-paleogeographic features of the Tarim basin during the Late Paleozoic are illustrated. The Devonian to Permian is an important period of terranes/island-arcs accretion and oceanic closure along the periphery of the Tarim block, and a critical period when the polarity of Tarim basin (orientation of basin long-axis) rotated at the maximum angle clockwise. During the Late Paleozoic, the periphery of the Tarim block was first collisional orogeny on its northern margin, followed by continuous collisional accretion of island arcs on its southern margin: on the Northern margin, the North and South Tianshan Oceans closed from East to West; on the South-Western margin, the Tianshuihai Island Arc gradually collided and accreted. These tectonic events reduced the extent of the seawater channel of the passive continental margin in the Western part of the basin until its complete closure at the end of the Permian. The Tarim basin was thus completely transformed into an inland basin. This is a process of regression and uplift. The Southwest of the Tarim basin changed from a passive to an active continental margin, through back-arc downwarping and eventually complete closure to foreland setting. The intra-basin lithofacies range from shelf-littoral to platform-tidal flat to alluvial plain-lacustrine facies. The tectonic-sedimentary evolution of the Tarim basin is strongly controlled by peripheral geotectonic setting.

KEYWORDS

Tarim basin, proto-type basin, tectono-paleogeography, Late Paleozoic, evolution

1 Introduction

As the largest interior basin in the world, Tarim basin is an outstanding natural laboratory to study proto-type basin and tectono-paleogeography. A clear determination of the proto-type basin of Tarim basin and its peripheral tectono-paleogeography can be useful to understand tectonic evolution of Paleo-Asian and Tethyan tectonic systems, to evaluate its resource potentials, and even to deduce the paleoclimate.

For these reasons, many studies have been performed to understand the dynamic evolution of basins and their relationship to paleogeography (Allen and Allen, 1990; Jia et al., 2004; Woodcock, 2004; Lin et al., 2012b; Ingersoll, 2012; Liu J. D. et al., 2014; Ingersoll, 2019). Numerous studies on tectono-paleogeography have also been performed in different areas and periods of the Tarim basin with different focuses: some focus on the development process of the Craton (Wang et al., 2017; Wang et al., 2019), some on the spatial and temporal spreading of the sedimentary facies' belts (Carroll et al., 1995; Zhang J. et al., 2007; Zhang J. et al., 2008; Wu et al., 2013; Li S. Z. et al., 2014; He et al., 2015) and some on the division of the stratigraphic sequence (Lin et al., 2009; 2012a; Zhao et al., 2009; Zhao et al., 2011). These studies have all made progress to varying degrees, and have provided guidance for hydrocarbon source rock evaluation and hydrocarbon exploration. However, due to the limited data or low accuracy, the maps compiled by different scholars in different periods have certain differences, mainly in the study area, sedimentary boundary, and microfacies distribution (Zheng et al., 2022). Moreover, with the progress of oil and gas exploration and development, there may still be some problems with these previous studies: 1) The previous paleo-plate tectonic patterns do not highlight the position of Tarim block. 2) The previous proto-type basin is only limited in the Tarim basin, lacking of overall analysis, and basin-mountain coupling processes. 3) The previous tectono-paleogeographic maps are still compiled in "fixed theory" (Feng et al., 2004; Hou et al., 2014). Therefore, it is necessary to carry out a new round of research on proto-type basin and tectono-paleogeography.

Based on numerous previous research results, the Tarim proto-type basins for each period of the Late Paleozoic were recovered using the latest field sections, drilling logs and seismic sections in this paper. In addition, the tectono-paleogeographic maps in each period were also given in conjunction with the investigation of peripheral plates of the Tarim basin to show the role of surrounding tectonic setting in controlling the basin interior. It is hoped that these maps will provide a basis for the interaction between the Tarim basin and the Paleo-Asian and Tethys tectonic systems, and provide fundamental supports for assessment of hydrocarbon exploration prospect in the Tarim basin.

2 Geological setting and plate tectonic configuration

The Tarim basin, a large-scale superimposed basin (Jia et al., 1997; He et al., 2007; Gao et al., 2017), is located in Central Asia, in the Xinjiang Province in China. It covers an area of 560×10^3 km^2 and is the largest inland basin in China. It can be divided by seven first-order tectonic units: the Kuqa Depression, the Tabei Uplift, the Northern Depression, the Central Uplift, the Southwest Depression, the Southeast Faulted Uplift, and the Southeast Depression (He et al., 2016). These seven first-order tectonic units are subdivided into 17 Secondary structural units (Figure 1A).

2.1 Tectonics and stratigraphy

Tectonically, the periphery of the Tarim basin underwent oceanic opening, subduction, oceanic closure, island arcs accretion, and collision processes during the Phanerozoic (Tapponnier et al., 2001; Xiao and Santosh, 2014). The processes reflect several phases of tectonism, magmatism, and metamorphism. Therefore, the tectonic environment around Tarim basin is quite complex (Figure 1A). The Tarim basin is separated from the Kazakhstan-Junggar block by the Tianshan Orogenic Belt to the North (Gao et al., 2013). The Tianshan Orogenic Belt is part of the Central Asian Orogenic Belt and is divided by two Paleozoic sutures (Windley et al., 1990; Allen et al., 1991; Ma et al., 2014) into three parts: the Northern Tianshan, Central Tianshan and Southern Tianshan. The Central Tianshan is also commonly referred to as the Yili-Central Tianshan Terrane together with the Yili block in the West (Allen et al., 1993). To the Southwest of the Tarim basin is the West Kunlun Orogenic Belt, which includes the North Kunlun, the Central, and South Kunlun, and the Tianshuihai Terrane (Zhang C. L. et al., 2019); to the Southeast are the Altyn-Qilian Island Arc, the Qaidam block, and Bayankala block. To the South are the North Qiangtang block, South Qiangtang block, Lhasa block and Himalayan Orogeny (Sobel and Dumitru, 1997; Pan et al., 2002).

Stratigraphically, the Tarim basin contains a pre-Sinian cratonic crystallized basement, above which a complete sedimentary sequence of the Sinian and Palaeozoic accumulated (Liu et al., 2016). During the Sinian and Paleozoic, marine calcareous, and terrigenous deposits were dominant until the Carboniferous (Laborde et al., 2019). A carbonate platform surrounded by passive continental margins and a deep shelf developed widely in the Cambrian and Ordovician, respectively. The Lower Silurian to Middle Devonian was dominated by sandstones of littoral deposits. A strong uplift event occurred in the late Middle Devonian, forming a regional unconformity (Figure 2) between the Middle and Upper Devonian. Shallow marine clastic rocks and limestone with biogenic limestone as interbeds occurred in the Carboniferous units (Li et al., 2015). The Permian sediments transition from bottom to top mainly from marine carbonates and sandstones to lacustrine or fluvial clastic rocks (Deledaer, 1996), with intervening volcanic rocks. After the Permian, marine deposition ceased in the Tarim basin with a change from calcareous to terrigenous deposits characterizing most of the Mesozoic sediments.

2.2 Plate tectonic configuration

The basis for recovering the proto-type basin and tectono-paleogeography is to understand the plate tectonic framework. Plate tectonic framework involves large-scale basin-mountain coupling and controls the formation and evolution of ocean-continent configuration, orogenic belts, and basins. Therefore, it can be used to reveal the process of ocean closure and orogenic uplift (Huang et al., 2023).

At present, most of the global plate tectonic evolution maps are reconstructed by Gplate software based on the global paleomagnetic database (Müller et al., 2018). However, large foreign plates are the

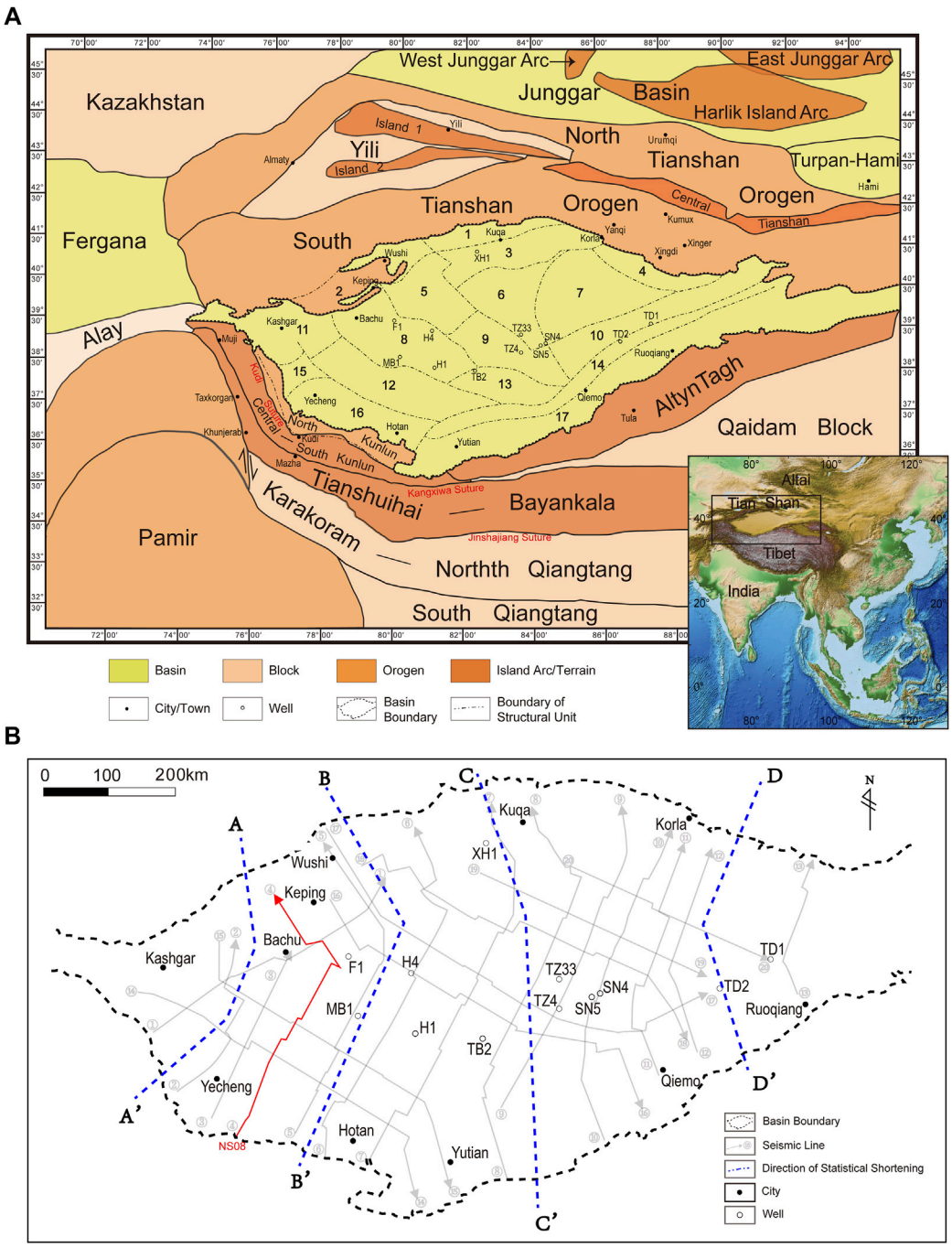

FIGURE 1
Schematic structural maps of the Tarim basin and adjacent areas, and location of the study area. **(A)** Schematic structural map of the Tarim basin and adjacent areas (modified after He et al., 2016); Structural units of Tarim basin: 1-Kuqa Depression; 2-Kalpin Faulted Uplift; 3-Tabei Uplift; 4-Kongque River Slope; 5-Awati Depression; 6-Shuntuoguole Uplift; 7-Manjiaer Depression; 8-Bachu Uplift; 9-Tazhong Uplift; 10-Guchengxu Uplift; 11-Kashi Depression; 12-Maigaiti Slope; 13-Tangguzibas Depression; 14-Tanan Uplift; 15-Shache Bulge; 16-Yecheng Depression; 17-Southeast Depression. **(B)** Location of 20 basin-scale seismic sections used to calculate shortening. These shortening data are integrated on four representative lines (AA', BB', CC', and DD') (cf. Laborde et al., 2019). The seismic section NS08 and the balanced cross-section recovered from it are shown in Figure 5.

priority core plates, and the three plates in China (Tarim block, North China block and South China block) are not paid enough attention.

The three plates in China should be constrained by high-confidence paleomagnetic data (Huang et al., 2008; 2018) and tectonic comparison in geological affiliation. The positions of the three plates in China can be appropriately adjusted on the same latitude, but they cannot be adjusted arbitrarily, and the spatial constraints between plates should be considered. The new global tectonic configuration in the Late Paleozoic is reconstructed by GPlate software based on the high-confidence paleomagnetic data (Huang et al., 2023).

In Devonian, the Tarim block, the North China Plate and the South China Plate were separated from the Gondwana continent and

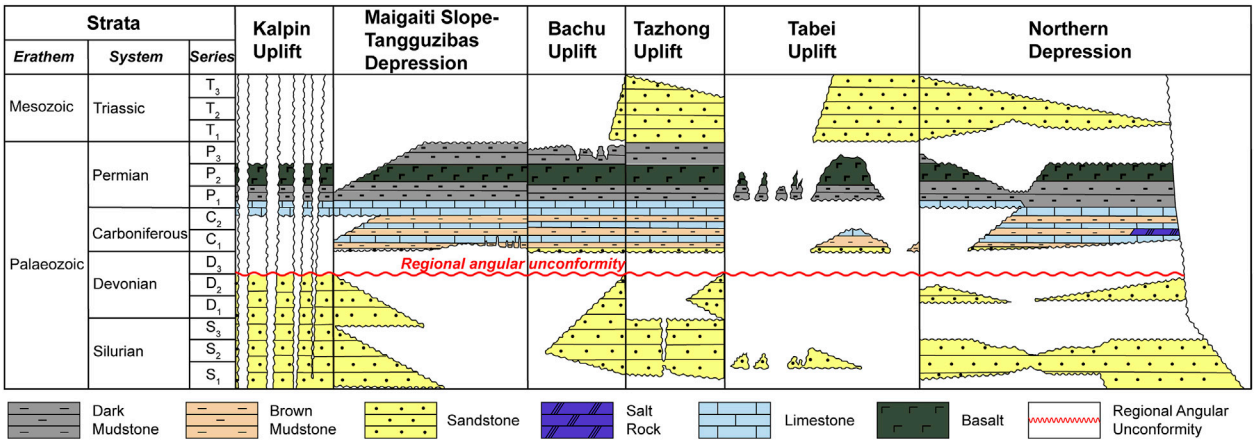

FIGURE 2
Silurian-Triassic tectonic-sedimentary evolution in the Tarim basin.

the Laurentia-Baltica-Siberia continent. The Tarim block was at around 15°N and formed a " $T\frac{N}{S}$" pattern with the North China Plate and South China Plate. The Tarim block was generally in a "Western compression, eastern extension" tectonic setting: the Paleo-Asian Ocean (Paleo-Tianshan Ocean) westward subducted under the Siberian-Kazakh continent, the Paleo-Asian Ocean domain was contracting, and the Southern Kunlun/Southern Altyn Ocean to the east was expanding (Figure 3A).

In Carboniferous, Gondwana, and Laurasia merged to form the main body of Pangaea, laying the foundation for the basic pattern of global plate tectonics (Figure 3B). The Tarim block drifted northwards to about 25°N and the Paleo-ocean (North and South Tianshan Ocean) on the northern edge of the Tarim block entered a period of major closure (Han et al., 2006; Wang et al., 2007; Charvet et al., 2011; Han and Zhao, 2018; Alexeiev et al., 2019). In the Late Carboniferous, Tarim block collided with Kazakh-Yili (Gao et al., 2009; Su et al., 2010; Han et al., 2011; Liu D. et al., 2014; Zhang et al., 2014a; Wang et al., 2022). By rotating clockwise, Tarim block gradually collided with Kazakhstan from east to west, forming the Kazakh Horseshoe Orocline (Abrajevitch et al., 2007; Görz and Hielscher, 2010; Li J. et al., 2014; Yi et al., 2015). At this time, the Tarim block ended its history of independent drift and became the southern edge of the Eurasian continent (Zhao et al., 2003; Xiao et al., 2008; Wilhem et al., 2012; Xiao et al., 2013). Tarim block regulated its position in relation to the other blocks in the Laurasia by rotating clockwise (Li et al., 2015).

During the Early-Middle Permian, the Western and middle segments of the Paleo-Asian Ocean had been closed, leaving only its Eastern segment unclosed. Tarim block joined the main body of Pangaea (Zhao et al., 2018). As a result of the crustal uplift caused by the late Hercynian tectonic movement, the seawater in the remnant bay of the Southwestern Tianshan area was gradually retreating Westward. The sedimentary environment within the basin also changed from marine to terrestrial (Chen et al., 2006; Luo et al., 2012; Zou et al., 2014). At the same time, the Tarim block produced intense volcanic activity, with large igneous provinces developing from 251 to 272 Ma. In the Late Permian (c. 270 Ma), Pangaea reached its largest scale, and was surrounded by the Panthalassa (Figure 3C). A series of orogenic belts, including the Central Asian Orogenic Belt and the Uralian Orogenic Belt, on the Laurasia and its periphery, resulting in the final assembly of Pangaea (Li and Jiang, 2013). At the end of the Permian, the Paleo-Asian Ocean closed completely (Eizenhöfer et al., 2014; 2015a; 2015b), the Paleo-Tethys Ocean subducted northwards and the Neo-Tethys Ocean began to spread. Tarim block was located to the north of the Paleo-Tethys Ocean and had been collaged with the Eurasian plate to the North. After the assemblage of Pangaea, the positions between the plates were adjusted by strike-slip faults. The Tarim block was adjusted by a large left-lateral strike-slip fault.

3 Methology and database

The proto-type basin analysis based on the thought of "mobile tectono-paleogeography", which includes basin resetting, restoration, and reshaping (Hou et al., 2019; He et al., 2020), is the core of this study. Basin resetting is to restore the geotectonic position of the proto-type basin in its development period. Basin restoration is to restore the initial status of the proto-type basin, including its scope and sedimentary facies distribution. Basin reshaping is to restore the superposition and modification processes, mainly the restoration of the amount of elongation/shortening of the basin.

Specifically, there are four steps in creating proto-type basin maps with tectonic background.

Firstly, replenishing the erosion thickness and restoring the intact isopach maps of the Tarim basin, which is mainly based on the residual strata thickness (Figure 4) from Bureau of Geophysical Prospecting, China, according to the characteristics of the sedimentary thickness trends in the different basins. The thickness trend method can find the boundary of the proto-type basin with the help of the trend of the isopach in the isopach map, and it can also be analyzed by the trend surface of a certain thickness layer in the seismic profile (Zhang X. B. et al., 2007; Yu et al., 2016).

Secondly, extending the intact isopach maps outwards based on the amount of shortening (Table 1) counted by 81 balanced cross-sections (Lou et al., 2016; Laborde et al., 2019) to restore the pre-deformation deposition extent and proto-type basin boundary.

Thirdly, restoring the distribution of lithofacies (intra-basin and marginal facies) according to lithofacies-paleographic maps and isopach maps. When the lithofacies-paleographic maps contradict

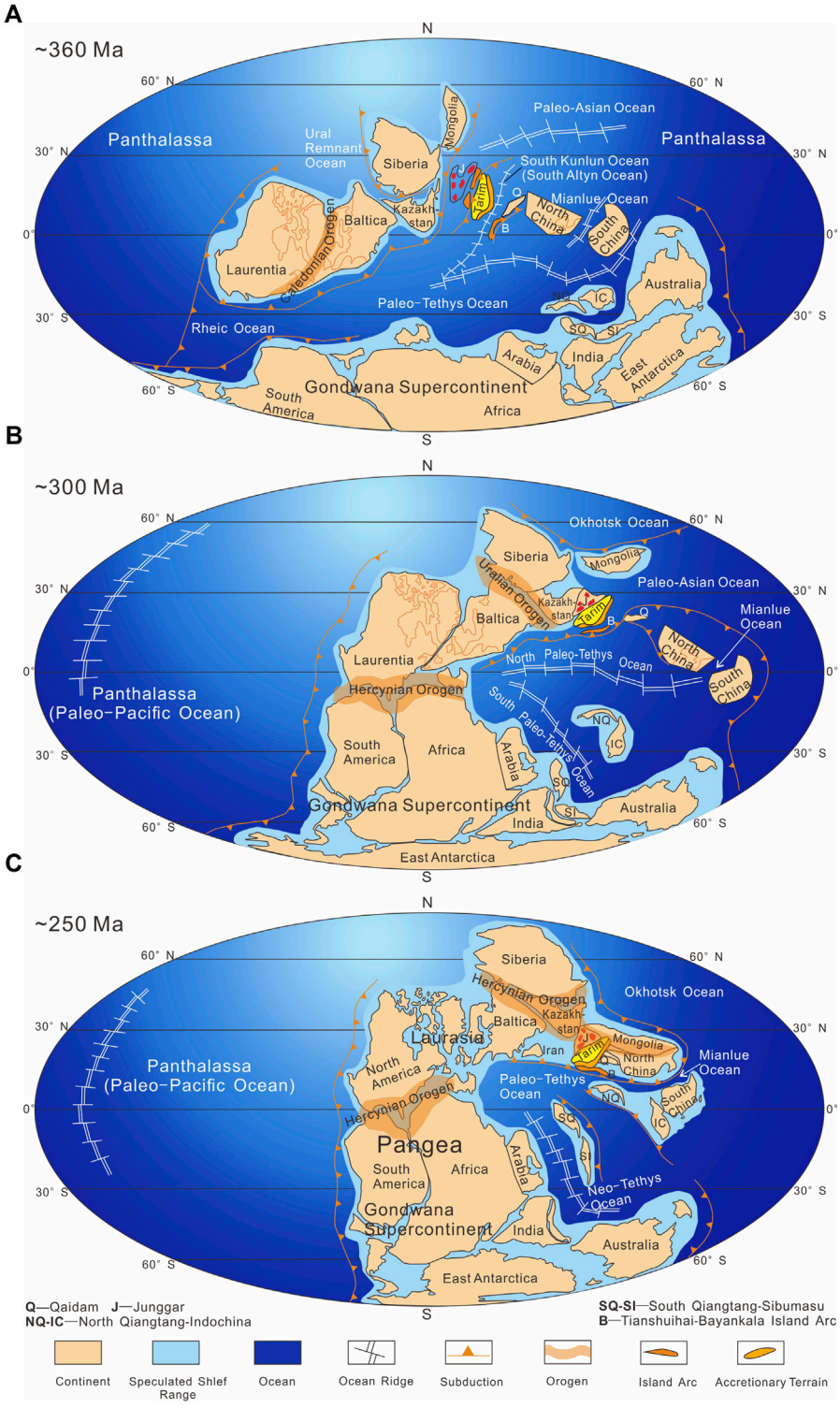

FIGURE 3
Reconstructing of global plates distribution in Devonian Period **(A)**, Carboniferous Period **(B)**, and Permian **(C)**.

the isopach maps, take the former as more credible due to the compilation of lithofacies-paleographic maps based on analysis of wells and outcrops in the whole basin.

Finally, completing the peripheral tectonic background of the Tarim basin according to the previous literatures and then obtaining the Tarim proto-type basin maps in the fourth chapter.

The maps compiled in this paper include two aspects: 1) The Tarim proto-type basin maps with peripheral tectonic setting under the current geographical coordinates in Late Paleozoic in the fourth chapter; 2) Tectono-paleogeographic maps of Tarim block and its peripheral areas under paleogeographic coordinates in Late Paleozoic in the fifth chapter.

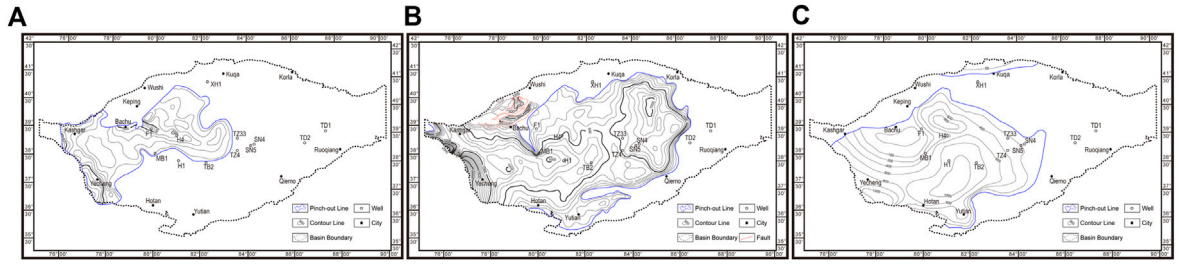

FIGURE 4
Residual strata thickness of Tarim Basin in Devonian Period **(A)**, Carboniferous Period **(B)**, and Permian **(C)**.

The data used in this study include: the residual strata thickness of Tarim basin from Devonian to Permian (Bureau of Geophysical Prospecting, China), lithofacies distribution maps of Tarim basin in different periods of Late Paleozoic, 81 seismic sections and their balanced cross-sections, and some information on drillings and outcrops. These basic data are mainly provided by the Tarim Oilfield Company.

3.1 The residual thickness of the Tarim basin

Bureau of Geophysical Prospecting INC. has completed a set of residual thickness maps (Figure 4) based on the fine interpretation of basic seismic horizons in the Tarim basin, combined with information from drilling and geological outcrops. These residual thickness maps are the basis for recovering the original thickness distribution of the basin prior to deformation.

Based on the residual strata thickness in Figure 4, according to the characteristics of different type basins, restore the intact isopach map. For a marginal basin, the isopach should be open, outward, and asymmetric. While for an intracratonic basin, the isopach should be concentric and closed. If encountering a platform or a surficial sea, then the isopach should be symmetrical but with openings connected to the shelf or marginal sea. For other kinds, their isopach maps should also be restored in accordance with their characteristics and locations in the Tarim block.

3.2 The amount of shortening of the basin

It is key work to calculate the shortening amount according to the balanced cross-sections in reconstruction of proto-type basin. The balanced cross-sections can provide information on the elongation/shortening of the strata (Lin et al., 2015; Wang et al., 2020a; Wang et al., 2020b). The restoration process for balanced cross-sections, where the mass conservation principle is the basic criterion, is usually inverse, i.e., starting from a current interpreted structural cross section to its pre-deformed morphology (Dahlstrom, 1969; Zhang and Chen, 1998). The stratum length balance restoration method and the area balance restoration method (Jiang et al., 2018) are used in this study. And the restoration process is carried out in 3D-MOVE software, including three steps: compaction correction, fault displacement restoration and layer leveling. The stratigraphic lengths and the amount of shortening in each period can be obtain after restoring the balanced cross-sections.

Figure 1B shows the positions of 20 basin-scale sections used in this study for the statistics of basin shortening data. Among them, 10 balanced cross-sections are restored by us. Here, the NS08 section is taken as an example to show the shortening process of the basin (Figure 5).

Because the deformation mainly exists along the margin of Tarim basin, the total shortening of each section is distributed to its two ends according to the ratio of deformation at both ends (Figure 6). These shortening data are integrated on four representative lines (AA', BB', CC', and DD') (Figure 1B; Table 1). The extension or shortening amount measured in this paper is from Devonian, Carboniferous, and Permian to Cenozoic. Data since the Cenozoic are referenced from Laborde et al. (2019).

The foreland (mountain front) zone is the main deformed part of the proto-type Tarim basin, with the largest proportion of Cenozoic shortening accounting for 70–90%. Overall, the distribution of shortening in the marginal segments of the Tarim basin shows a certain regularity: the shortening decreases from west to east, which is probably due to the increasing distance from the Pamir tectonic syntax.

4 Reconstruction of Tarim proto-type basin in the Late Paleozoic

4.1 Late devonian: A back-arc extensional basin in the southwestern Tarim basin

In the Early-Middle Devonian, Tarim basin basically inherited its Silurian sedimentary framework (Li et al., 2015). By the end of the Middle Devonian, the Early Hercynian Movement made the Tarim basin strongly uplifted and subjected to denudation and planation, forming a regional angular unconformity (Liu et al., 2008) (Figure 2) between the Middle and Upper Devonian. The tectonic framework of the Tarim basin undergone important changes as a result of the Early Hercynian movement (Huang, 1986; He et al., 2005; Li et al., 2015; Wu et al., 2016), which made the basin present a tectonic environment of "compression in the northeast and southeast, extension in the southwest" (Figure 7A). The northeast and southeast of Tarim basin uplifted strongly, forming the denudation areas in these regions (Figure 7A). The compression from these two directions caused the basin to tilt uplift from East to West, showing a pattern of "Eastern uplift, Western depression" (Lin et al., 2012b), and seawater mainly invaded the basin from the West (Hu et al., 2010; Ma et al., 2019). The

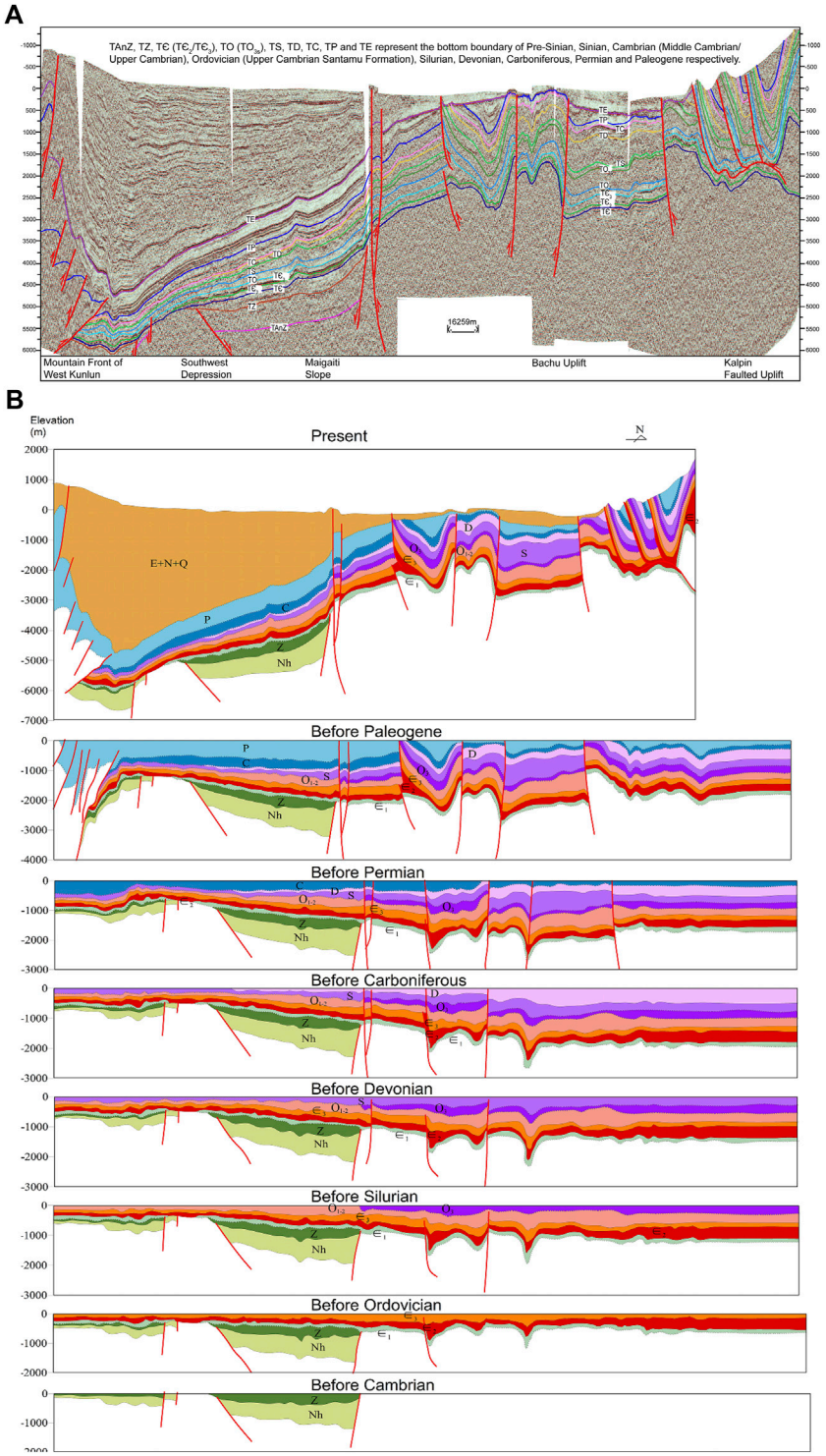

FIGURE 5
Geological interpretation of seismic section NS08 **(A)** and its recovered balanced cross-section **(B)**. The location of seismic section NS08 is shown in Figure 1.

Southwest of Tarim basin changed from passive continental margin to back-arc extensional environment (Figure 7A).

There were several inherited paleo-uplifts in the basin, including Shaya Uplift in the North, Tadong Uplift in the East and Tanan Uplift in the South (Chen, 2000). The basin formed an open-sea basin with Westward opening and a tectonic depressive bay basin centered on the Awati Depression (Ma et al., 2019) (Figure 7A).

It is controlled by the paleo-geomorphic background that the shelf-shore facies (Liu et al., 2016) were mainly developed in the basin from West to East (Figure 7A). Tarim basin was surrounded by shallow

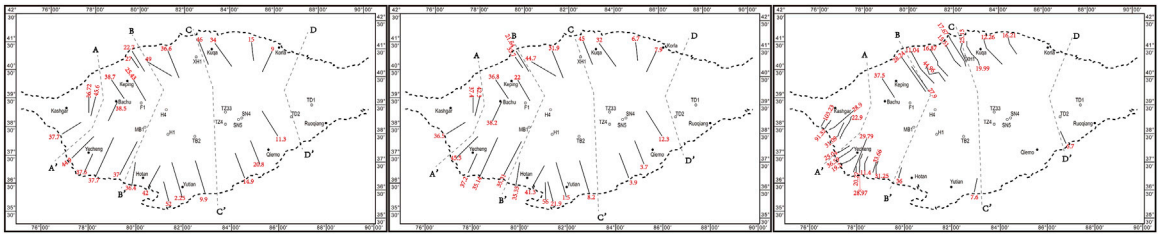

FIGURE 6
Distribution of shortening at the basin margin calculated from each seismic section.

continental shelf, the Western part of which was relatively open with huge thickness turbidite clastic rocks (Lin et al., 2011). From west to east, the sedimentary environment showed a changing trend from shelf-shore to backshore-delta around the paleo-uplift (Figure 7A). Shelf facies mainly developed gray-green mudstone intercalated with thin siltstone, shore facies mainly developed tabular cross bedding and low angle cross bedding quartz sandstone (Zhang H. et al., 2009). Delta facies developed in well TB2 and estuarine facies developed in well TZ4 (Xu, 2009; Jia et al., 2017) (Figure 7A). Marginal facies such as deltas (Figure 7A) indicated the boundaries of proto-type basin and the major provenance areas. The quartz sandstone of the lower sandstone section of the Donghetang Formation was deposited in the Bachu-Maigaiti area. The Kalpin paleo-uplift in the North and the Madong paleo-uplift in the South provided sufficient clastic materials, forming a shelf-shore sedimentary system, and the sand body sedimentation gradually migrated Eastward (Su, 2019). The H1 well area received provenance from the southern paleo-uplift in the basin (Figure 7A), and developed gravelly shore facies (Zhu et al., 2016). The Kuqa area received the provenance from the Tabei paleo-uplift and the Xingdi area (Su, 2019).

It is the tectonic background around the basin that controlled the above phenomena in the basin. On the periphery of the basin, the eastern segment of the South Tianshan Ocean began to shrink and the western segment was still expanding (Figure 7A). The Central-South Kunlun Island Arc, which was collaged to the southwestern margin of the Tarim basin at the end of the Early Paleozoic (Matte et al., 1996; Zhang Y. et al., 2019), was a low underwater uplift (Figure 7A). The Southern Kunlun Ocean lied between the continental margin of the Southwest margin of Tarim basin and the Tianshuihai Island Arc, which began to move to the southwest of the Tarim basin. The Altyn-Qilian Island Arc, which was collaged to the Southeast edge of Tarim basin at the end of the Early Palaeozoic (Xu et al., 2011), had become a part of the Southeast Uplift. The Southern Altyn Ocean, which existed between the Altyn—Qilian Island Arc and Qaidam block, subducted northward, causing the Southeastern Tarim basin to continuously uplift (Figure 7A).

4.2 Late carboniferous: Transition from a back-arc extensional basin to a back-arc downwarping basin in the southwestern Tarim basin

From the beginning of Carboniferous, the Tarim block generally subsided and undergone extensive marine transgression (Zhuang et al., 2002; Ma et al., 2019). There were marked differences in the paleogeography and the width of the sedimentary facies expressed due to their location (Figure 7B).

The range of the proto-type basin changed significantly (Figure 7B). The boundary of the proto-type basin in the East starting from the Westernmost part of the Kongque River Slopes, passing through the Manjiaer Depression to the south and reaching the Guchengxu Uplift. At the junction of the south side of Guchengxu Uplift and the Southeastern Fault-Uplift, the boundary turned

TABLE 1 Shortening amount of Tarim Basin between Devonian, Carboniferous, Permian Periods and present (/km).

Distribution of the shortening amount	Cenozoic Period	Devonian Period	Carboniferous Period	Permian Period
North margin of AA'	36.00	39.88	38.68	37.50
South margin of AA'	32.00	41.30	41.00	36.68
North margin of BB'	21.00	31.03	30.51	25.80
South margin of BB'	35.00	40.43	40.05	36.00
North margin of CC'	22.00	38.87	36.30	17.80
South margin of CC'	0.90	9.02	8.88	7.60
North margin of DD'	~0	12.00	7.30	~0
South margin of DD'	0.30	16.05	8.00	6.70

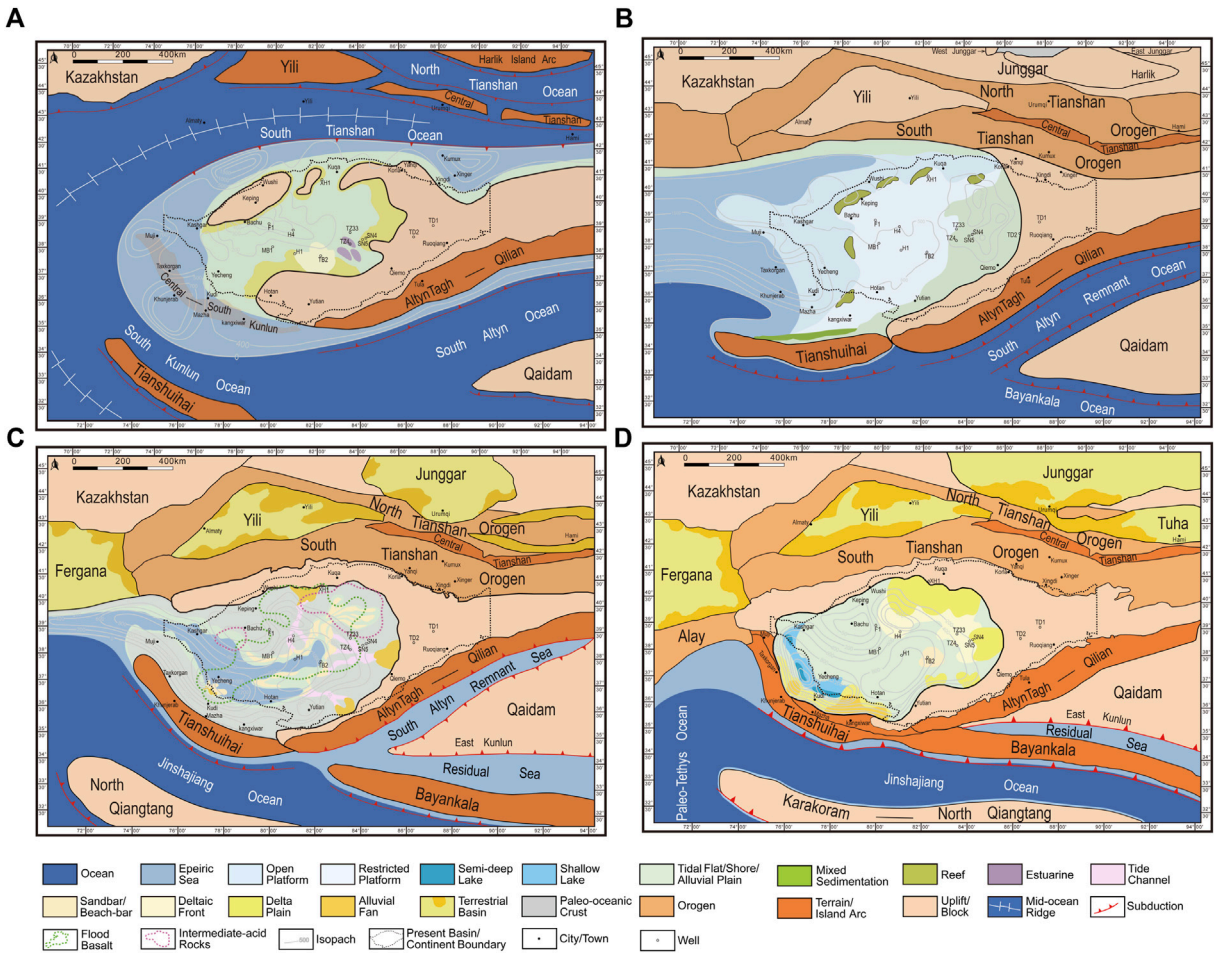

FIGURE 7
Proto-type basin of Tarim and adjacent areas in late Devonian **(A)**, late Carboniferous **(B)**, late Middle Permian **(C)** and late Permian **(D)**.

southwest and basically extended parallel to the Southeastern Fault-Uplift to the southern Tarim basin.

In terms of the Uplift-Depression Framework, the entire Tarim basin still maintained the overall geomorphology of high in the East and low in the West (Xie et al., 1997; Zhang G. et al., 2007) (Figure 7B), specifically manifested as ring uplifts in the North, East, and southeast (Li et al., 2015), and depressions in the central and Western regions (Figure 7B). The Northeast of the basin was the main denudation area. The middle part was an intracraton depression (Zhang G. et al., 2007), with stable sedimentation.

Within the Tarim proto-type basin, the large areas (such as Kuqa Depression, Shaya Uplift, and Kalpin Uplift) West of the Kongque River Slopes in the Northern part of the basin were submerged due to the transgression from Southwest to Northeast (Xie et al., 1997) (Figure 7B). The area with larger relative water depth was in the west of Kuqa Depression. The water depth of Shaya Uplift to the South was relatively shallow. In general, the basin developed interactive marine and terrestrial deposits and marine carbonate rocks deposits (Carroll et al., 1995) (Figure 7B). The Carboniferous System was generally 500–1000 m thick, and its loss in Eastern and Southeastern Tarim basin was caused by uplift and denudation in the late stage (He et al., 2005; Wu et al., 2020).

From East to West, tidal flat facies, restricted platform facies, open platform facies, and shallow marine shelf facies developed in sequence (Ye et al., 1997; Pu et al., 2014) (Figure 7B). The tidal flat facies developed in the Eastern part of the basin were in the form of NE-SW trending strips, the width of which was greater within the Guchengxu Uplift and the Manjiaer Depression (Figure 7B). The tidal flat facies mainly developed mudstone and limestone during the sedimentary period of Xiaohaizi Formation (Gu et al., 2003). For example, the Xiaohaizi Formation of well TZ33 drilled limestone with a single layer thickness of more than 5 m and mudstone with a relatively thin layer thickness. The restricted platform facies had the largest distribution range, occupying most of the central Tarim basin (Figure 7B). The lithology of restricted platform facies was mainly gray thin-layer mudstone and medium-thick layered limestone, with argillaceous limestone developed locally. On the outside of the restricted platform, there was the band-shaped high-energy facies (Xu, 2009) with unstable width between the restricted platform and the open platform (Figure 7B). The high-energy facies band in the platform had an S-shaped trend, which might be related to the two finger-shaped residual bays left in the west and southwest of the Tarim basin (Figure 7B). In the high-energy zone, the platform margin reef was mainly developed along the S-shaped platform margin (Guo et al., 2018), and its lithology was mainly bioclastic limestone. The outside of the high-energy zone was open platform facies, which

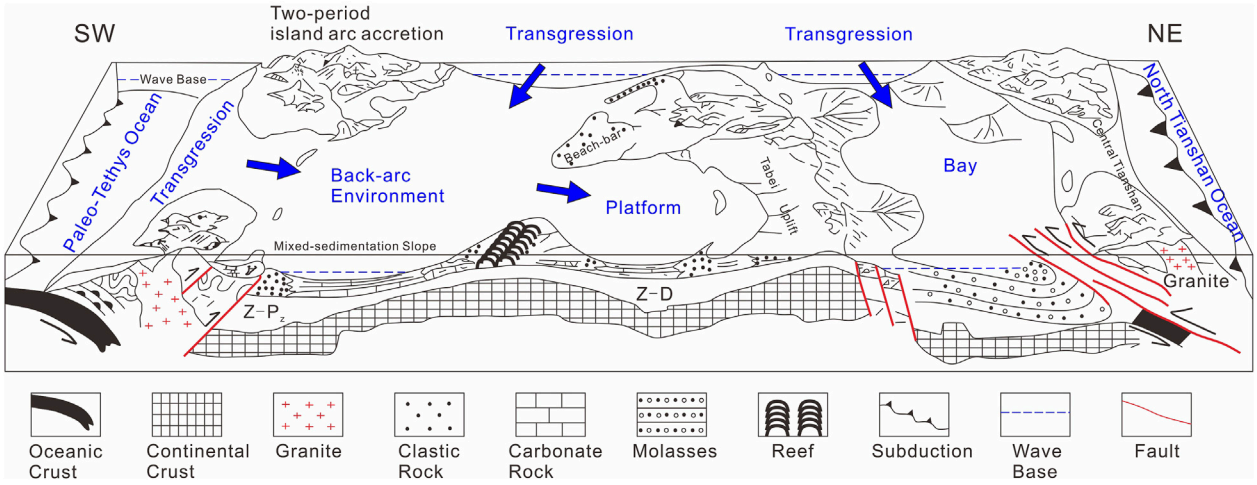

FIGURE 8
Carboniferous-Permian proto-type basin configuration in Tarim basin (modified according to He et al., 1992; Gong, 2010; Zhou et al., 2014).

was mainly composed of continuously deposited thick layers of limestone (dolomite), but generally mud rocks were not developed (Qi et al., 2020). There was a mixed sedimentation zone (Figure 7B) in Southwest of the Tarim basin, which was similar to the foreland basin on the Eastern side of the Andes.

The Tianshuihai Island Arc began to collage and approach, but it had not completely closed the Tarim basin (Figure 7B). The South Kunlun Ocean shrinked further and was close to almost closure. The Southwestern Tarim basin changed from a back-arc extensional basin to a compressive downwarping basin. Currently, the Southwestern margin of the Tarim basin was the active continental margin (Li et al., 2015) (Figure 8). The residual ocean of the South Altyn lied between the Qaidam and Tarim block. The subduction zones in the north and south of Qaidam block were both subducted towards it (Figure 7B).

4.3 Late Middle Permian: Transition from back-arc flexural basin to foreland basin

Since Permian, large-scale regression occurred in the western Tarim basin (Liu et al., 1994; Liu X. et al., 2014), and the eastern Tarim basin became the uplift erosion area. During the Middle Permian, the Paleo-Tethys Ocean south of the Kangxiwar Fault continued to subduct to the Tarim block (Hofmann et al., 2011; Yang et al., 2011; Liu K. et al., 2014; Zhang Y. et al., 2019) (Figure 7C), which further developed the southwest back-arc flexural basin. Increased orogenic activity in the northern Tarim block uplifted the eastern and northern parts of the basin, accompanied by large-scale intermediate-acid volcanic magmatism (Liu et al., 2016) (Figure 7C).

The range of the proto-type basin changed greatly (Figure 7C). From the north side of the Kalpin Fault-Uplift to the east, including most of the Kuqa Depression and the eastern Shaya Uplift were uplifted and exposed to erosion. East of the central part of the Manjiaer Depression, the central part of the Guchengxu Uplift and most areas east of Southeastern Fault-Uplift were uplifted and eroded (Qi et al., 2020). Overall, the Tarim basin was surrounded by a semi-enclosed uplift in the northwest, north, east, and southeast, along with an island arc belt developed in the southwest, as a residual epeiric sea that might open only in the west (Zhu et al., 2007) (Figure 7C).

The central and eastern Tarim basin in the Middle Permian was a westward sloping intra-cratonic depression basin (Chen X. et al., 2013). The paleo-geomorphological features were generally shallow in the southeast and deep in the northwest, with the greater water depth in the NE-E direction.

A set of residual shallow sea and tidal flat deposits were developed in the western basin (Ye et al., 1997) (Figure 7C). The residual shallow sea was mainly developed in the southwest of the basin, extending eastward into two branches (Figure 7C). The northern branch extended northeast to the eastern part of the Madong Thrust Belt, and the southern branch extended eastward to the western part of the Southeastern Fault-Uplift. Alluvial fans of varying sizes developed within the mud flat deposits. Typical wells drilled in mixed flat deposits, such as well SN5, were dominated by mudstones and silty mudstones, interbedded with thin to medium bedded fine sandstones and gravel-bearing fine sandstones (Qi et al., 2020). Banded mixed-flat deposits were developed between residual shallow sea and mud flat. At the same time, beach sandbars were more developed in the mixed flat, especially in the frontal area of the braided river (Figure 7C). The emergence of the thousand-meter continental molasse (He et al., 2005) in the Duwa Formation in southwestern Tarim basin indicated that a back-arc foreland basin was formed in southwestern Tarim basin (Zou et al., 2014; He, 2022).

Besides sedimentary rocks, plenty of magmatic rocks were developed in the western part of Tabei Uplift, Bachu Uplift, Tazhong Uplift, Southwest Depression, Awati Depression and western Manjiaer Depression, and their rock types mainly included basic basalt, diabase, gabbro and alkaline syenites (Liu et al., 1994; Chen et al., 2006).

4.4 Late permian: A closed terrestrial intra-cratonic basin in whole

At the end of Permian, the Southern Tianshan area was completely orogenic uplift with the shrinkage of the residual sea in the southwest Tianshan area (Carroll et al., 1995). Alay area uplifted and transformed into an orogenic belt (Figure 7D). At the same time, Tarim basin was fully integrated into the Paleo-Eurasia continent (Zhao et al., 1990), and only the Paleo-Tethys Ocean existed on its South side. The continuous Northward subduction of the Paleo-Tethys Ocean (Xiao et al., 2003; Schwab et al., 2004; Robinson et al., 2007; Zhang Y. et al., 2019; Zhang et al., 2020) resulted in the complete collage and collision of the Tianshuihai Island Arc with the Tarim block (Li H. et al., 2014), which eventually closed the opening of the Western Tarim block (Figure 7D). Therefore, the main characteristics of the paleogeographic pattern of Tarim block and its surrounding areas in the Late Permian were that the sea water had completely retreated, and Tarim basin became a closed terrestrial intra-cratonic basin in whole (He et al., 2013; Ma et al., 2019) (Figure 7D).

Compared with the Late Carboniferous and Middle Permian, the proto-type basin at the end of the Permian was narrowed in the southwest (Figures 7C, D). In the Southern part of the basin, the proto-basin marginal uplift extended Westward. The proto-type basin in the east is basically bounded by the large uplift area.

The continuous uplift in the southeastern Tarim basin resulted in great changes in the uplift-depression framework of the Late Permian. Specifically, the paleogeomorphology changed from the former marine facies and residual marine facies of "high in the east and low in the west" into the closed lacustrine facies (Qi et al., 2020). Geomorphologic features also showed the typical lake-basin landscape of "high at the edge and low in the middle". The area with the greatest water depth was distributed in NW-SE direction.

At the end of Permian, lacustrine facies—lacustrine delta facies—coastal plain facies deposits were mainly developed in the Tarim basin (Zhu et al., 2007) (Figure 7D). There were narrow lacustrine deposits only in the southwest of the basin (He et al., 2013). There were deltas/fan deltas deposits on the inner edge of the basin, and the rest of the basin was alluvial plain. Three provenance systems were mainly developed in the North, East, and Southwest of the basin (Chen S. et al., 2013). The delta in the Northern part of the basin was a large delta system composed of overlapping delta lobe bodies. The delta front could be pushed southward to the Southern part of Awati Depression and the central part of Shuntuoguole lower uplift. In the Eastern part of the basin, a nearly EW-trending delta system was developed (Figure 7D), and the deltaic front could move westward to the central region of the Katake Uplift. Typical well drilled in this delta deposit was SN4 well. In addition, a relatively large deltaic front beach bar sand body (Figure 7D) was also developed outside the delta front (central area of Tanggubasi Depression). There were three semi-deep lake areas in Southwestern Tarim basin, which might be potential source-rock development areas.

In summary, the Tarim basin was in the regional tectonic background of plate convergence during the Carboniferous-Permian, a transitional stage from plate spreading regime to plate collision regime. The Northern Tarim basin became a foreland basin (Carroll et al., 1995) due to the closure of the Southern Tianshan Ocean. In contrast, the Southwestern Tarim basin entered a period of transition from a back-arc extensional basin to a foreland basin through a downwarp basin, and was by no means an open passive continental margin (Figure 8), as supported by the mixed coastal-clastic shore facies deposited here. Only the extensive sea shelf existed as a seawater channel in the western part of the Tarim basin. The Carboniferous-Permian basin genesis of the Southwestern Tarim basin was relatively similar to the Cenozoic Western Pacific trench, arc and basin system.

5 Reconstruction of tectono-paleogeography around the Tarim basin

Tectono-paleogeography is an important part of the research in multicycle superimposed sedimentary basins. Evolution of sedimentary basins is closely related to surrounding tectonic setting (Zhang et al., 2016; Wu et al., 2020). In reverse, the study of tectono-paleogeography can provide feedback for the proto-type basin analysis above to see if there are any improprieties. Sorting out the late Paleozoic tectono-paleogeography evolution of Tarim basin can offer an intuitive picture of how Tarim basin and its surrounding areas evolved and the tectonic factors driving these evolutions.

The tectono-paleogeographic maps in paleo-latitudinal coordinates have a range between the global plate tectonic maps and the proto-type basin maps and are integrations of the two.

Firstly, the proto-type basin maps are rotated in accordance with the paleolatitude and long axis direction of the Tarim block in the global plate maps. Then, the range of the span of about 30° latitude and 40° longitude is selected in this paper. According to the paleogeographic spatial pattern of the Tarim block and its surrounding plates, the proto-type basin maps are extended outwards to the periphery of the basin under the paleolatitude geographical coordinates. Finally, the paleogeographic information of the peripheral plates is supplemented to compile the tectono-paleogeographic maps of the Tarim block for each period.

5.1 Devonian tectono-paleogeography

In Devonian, the Tarim block was independently dissociated between the Gondwana continent and Siberia-Kazakhstan continent (Figure 9A). Siberia and Kazakhstan were separated by the ocean and were not yet united as a continent (Windley et al., 2007). The southeastern edge of Siberia and the eastern edge of Kazakhstan were shallow-sea continental shelf (Golonka et al., 2006; Zhang G. et al., 2019) (Figure 9A). Siberia and Kazakhstan were approaching Tarim block due to subduction of the Paleo-Asian Ocean, while Junggar Island Arcs were between the Siberia- Kazakhstan and Tarim blocks (Xiao et al., 2009; Carmichael et al., 2019). The North and South Tianshan Oceans were both subducted bidirectionally (Charvet et al., 2011; Ge et al., 2012; Guo et al., 2013; Han and Zhao, 2018).

The Western side of the North Tianshan Ocean subducted beneath the Harlik Island Arc (part of the Chinese North Tianshan Arc system) (Carmichael et al., 2019; Zhang et al., 2021), while the Eastern side subducted eastwards beneath the Yili-Central Tianshan Island Arc (Ren et al., 2017). In addition, the Southern Tianshan Ocean also subducted westwards (Figure 9A), resulting in the both

sides of the Yili-Central Tianshan Island Arc were clipped under the subduction zone and continued to develop (Han and Zhao, 2018; Huang et al., 2020).

The South Tianshan Ocean tended to close in the north, but it was still expanding in the South. It was shaped like a "bell-mouth" with the opening facing South (Figure 9A). In the eastern part of the Tarim block, the Central-South Kunlun and Altyn Island Arcs collided with the Tarim block as early as the end of the Ordovician due to the Late Caledonian Movement (He et al., 2011; Zhang et al., 2015; Dong et al., 2018). The Central-South Kunlun Island Arc was already submerged, with a wide passive margin to its southeast, across the South Kunlun Ocean from the Tianshuihai Island Arc (Dong et al., 2021) (Figure 9A). The South Altyn ocean subducted to the west, contracting the oceanic domain and causing continued uplift to the southeast of the Tarim block. The Tianshuihai Island Arc and Qaidam block were in a "Western extension, Eastern compression" tectonic environment, with the north-western side of the Paleo-Tethys Ocean subducting beneath the Tianshuihai Island Arc and Qaidam block (Figure 9A). In terms of land-sea framework, the Southern and Southeastern edges of Qaidam block and the Southwestern edge of North China plate were shallow-sea continental shelf (Figure 9A), and there was an ocean between Qaidam block and North China plate (Golonka et al., 2006; Li et al., 2018).

5.2 Carboniferous tectono-paleogeography

The tectono-paleogeographic map (Figure 9B) of the Tarim block at the end of Carboniferous showed that with the clockwise rotation of Mongolia, the middle part of the Paleo-Asian Ocean in southern Mongolia contracted, and the Southern edge of Mongolia was shallow marine environment (Hou et al., 2014; Liu et al., 2017). The Ural Ocean closed and formed orogenic belt (He et al., 2013). The Kazakh and Siberian plates collided, with the Siberian Sea remaining between them (Figure 9B). The southern part of Kazakhstan was shallow-sea continental shelf, and the gulf extended to the central part of Kazakhstan (Wan and Zhu, 2007), with lake basins developed on the continent (Ma et al., 2020). Affected by the closure of the North and South Tianshan Ocean (Charvet et al., 2011; Alexeiev et al., 2019) and the collision between Tarim block and Yili-Central Tianshan Island Arc (Han et al., 2011; Liu D. et al., 2014; Zhao et al., 2018; Wang et al., 2020), the oceanic crust of the Junggar arc system disappeared and the new continental crust was formed, but shallow sea remained overlying (Figure 9B). In Southwestern Tarim block, the demise of the South Kunlun Ocean caused the Tianshuihai Island Arc to begin colliding with the Tarim block. The Northern, Eastern, and Southern parts of Tarim block were raised in a half-ring shape, forming a sea basin that opened to the West. As the Southwest Tianshan did not completely close (Liu et al., 1994; He et al., 2005), the remaining remnant bay connected with the shallow sea in the Southern Kazakhstan through the Western opening of Tarim block (Figure 9B). To the South of the Tianshuihai Island Arc, the Paleo-Tethys Ocean subducted towards Tarim block (Zhang et al., 2022), resulting in the Southern Tarim block being an active continental margin (Figure 9B). Between Qaidam and Tarim block was the South Altyn Remnant Ocean, and the subduction belts existed on both the north and south sides of the Qaidam block (Figure 9B).

5.3 Late Middle Permian tectono-paleogeography

The Middle Permian tectono-paleogeographic map (Figure 9C) of the Tarim block showed that the Kazakhstan inherited its late Carboniferous pattern (Van der Voo et al., 2006). On the one hand, the southward subduction of the Okhotsk Ocean closed the middle part of the Paleo-Asian Ocean in the south of the Mongolia plate to form the residual sea (Figure 9C); on the other hand, due to the convergence and compression, the Junggar and Tianshan Orogenic Belts were integrated into the magnificent Central Asian Orogenic Belt (Figure 9C). The Tarim block continued its clockwise rotational adjustment. The remnant bay in the Southwest Tianshan region disappeared (Carroll et al., 1995) and the Fergana and Yili area developed into terrestrial basins (Clarke, 1984; Moisan et al., 2011). The Paleo-Tethys Ocean continued to subduct northwards (Cocks and Torsvik, 2013; Xiao et al., 2013), resulting in continuous collision between the Tianshuihai Island Arc and the Tarim block (Zhang Z. et al., 2009). The west opening of Tarim block was further closed, and only a narrow channel (Figure 9C) was left as the channel for the withdrawal of seawater. The North and South sides of Qaidam-North Qilian block were both remnant sea, and the Bayankala Island Arc in the South was approaching to the north. North China plate also joined the Pangea supercontinent and was surrounded by shallow-sea continental shelf (Zhao et al., 2018). Central North China and Western Mongolia were lacustrine facies (Figure 9C), and there were shallow marine facies between North China and Mongolia plate (Jolivet, 2015; Niu et al., 2021). The North Qiangtang block was in a shallow marine environment (Hou et al., 2014; Zhang G. et al., 2019) between the Eastern Paleo-Tethys Ocean and Mianlüe Ocean.

5.4 Late Permian tectono-paleogeography

As shown in Figure 9D, the Central Asian Orogenic Belt continued to increase in size as the withdrawal of seawater and uplift orogeny in southern Kazakhstan at the end of the Permian (Korobkin and Buslov, 2011; Ma et al., 2020). A remnant marine environment lied between the Iranian plate and the Fergana basin (Figure 9D). The range of uplift of the Mongolia plate also increased, with only a bay remaining to its east. At the same time, the Alay uplift orogeny (Gao et al., 2019) completely withdrew the seawater from the Tarim basin, which was thus transformed into terrestrial deposits (Carroll et al., 1995; Chen et al., 2006; He et al., 2013; Zou et al., 2014; Li et al., 2021). There were lacustrine deposits in the southwest of the Tarim basin (Figure 9D), and the peripheral foreland basin was generally developed. North China plate collided with Mongolia plate (Zhao et al., 1990) and the Qaidam-Qilian block had also been collaged with the Tarim block (Jolivet, 2015) (Figure 9D). Blocks such as Qiangtang in the south pushed northwards (Song et al., 2015; Xu et al., 2015; Hu et al., 2022; Ju et al., 2022), and the Paleo-Tethys Ocean continued to subduct beneath the Eurasian continent to the North (Pullen et al., 2008; Xiao et al., 2013; Yan et al., 2016; Li et al., 2020).

In conclusion, the Tarim block maintained clockwise rotation in the Late Paleozoic (Figures 9A–D), and the rotation angle of the Tarim block in the Late Paleozoic is much more than the other periods.

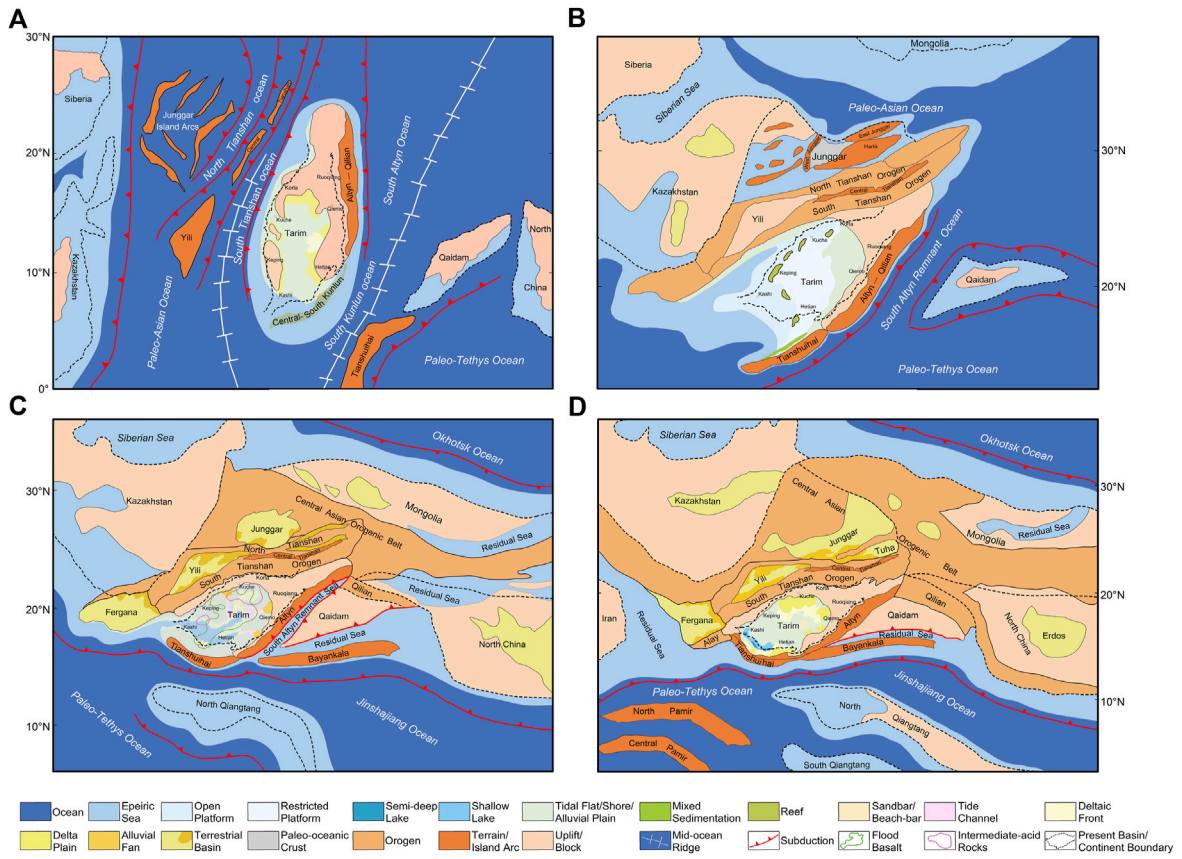

FIGURE 9
Tectono-paleogeography of Tarim and adjacent areas in late Devonian **(A)**, late Carboniferous **(B)**, late Middle Permian **(C)** and late Permian **(D)**.

6 Conclusion

1) The evolution of the proto-type Tarim basin is strongly controlled by the geotectonic setting of the periphery. The transition from shelf-littoral to platform-tidal flat to alluvial plain-lacustrine facies in the basin reflected a process of regression and uplift. This process was controlled by the shift in the peripheral tectonic setting of the basin: the North Tianshan Ocean and South Tianshan Ocean closed from east to west; the Tianshuihai Island Arc gradually collaged to the southwest of the Tarim block, reducing the extent of the opening of the passive margin of the western Tarim basin and closing it completely by the end of the Permian, resulting in the complete transformation of the Tarim Basin from a westward-opening marine basin to a terrestrial intra-cratonic basin.
2) The Southwestern Tarim basin was by no means an open, extensive passive margin during the Carboniferous-Permian, but rather transformed from a passive continental margin to an active continental margin through back-arc downwarp and eventually complete closure to uplift.
3) The Tarim block was located between 15°–25° N in the global plate tectonic framework in the Late Paleozoic. The Tarim block ended its independent drift to become the southern edge of the Eurasian continent at the end of the Carboniferous. The Tarim block witnessed and participated in the assemblage of the Pangea supercontinent. Meanwhile, its polarity (orientation of basin long-axis) underwent a significant clockwise rotation—from NNE to NE, which is associated with the closure of the Paleo-Asian Ocean from West to East to form the Central Asian Orogenic Belt.
4) As a result of the global Hercynian Orogeny Movement, the Tarim block and its surrounding tectonic setting underwent a major transformation: the Paleo-Asian Ocean and Paleo-Tethys Ocean closed in succession (the South Tianshan ocean completely closed at the end of the Carboniferous, the South Kunlun Ocean and South Altyn Ocean closed at the end of the Permian), followed by arc-continent collision and continental collision. The Tarim basin transitioned from a back-arc extensional basin to a back-arc foreland basin.

Data availability statement

The datasets presented in this study can be found in online repositories. The names of the repository/repositories and accession number(s) can be found in the article/Supplementary Material.

Author contributions

JX undertook most of the main work of this paper, including data collection, analysis, balanced profile restoration, manuscript writing, drawing maps, and so on; ZZ, XL performed some analysis work; SH, CL, and HL provide information and some maps; HC, LW: investigation. All authors contributed to manuscript read, and approved the submitted version.

Conflict of interest

SH, CL, and HL were employed by Institute of Petroleum Exploration and Development, Tarim Oilfield Company.

The remaining authors declare that the research was conducted in the absence of any commercial or financial relationships that could be construed as a potential conflict of interest.

Publisher's note

References

Abrajevitch, A., Van der Voo, R., Levashova, N. M., and Bazhenov, M. L. (2007). Paleomagnetic constraints on the paleogeography and oroclinal bending of the Devonian volcanic arc in Kazakhstan. *Tectonophysics* 441 (1-4), 67–84. doi:10.1016/j.tecto.2007.04.008

Alexeiev, D. V., Biske, Yu. S., Djenchuraeva, A. V., Kröner, A., and Getman, O. F. (2019). Late carboniferous (kasimovian) closure of the South Tianshan Ocean: No triassic subduction. *J. Asian Earth Sci.* 173, 54–60. doi:10.1016/j.jseaes.2019.01.021

Allen, M., Windley, B., Chi, C., Zhong-Yan, Z., and Guang-Rei, G. (1991). Basin evolution within and adjacent to the tien Shan range, NW China. *Jgs* 148, 369–378. doi:10.1144/gsjgs.148.2.0369

Allen, M., Windley, B., and Zhang, C. (1993). Palaeozoic collisional tectonics and magmatism of the Chinese Tien Shan, central Asia. *Tectonophysics* 220, 89–115. doi:10.1016/0040-1951(93)90225-9

Allen, P. A., and Allen, J. R. (1990). *basin analysis: Principles and applications*. London: Blackwell Scientific Publication.

Carmichael, S. K., Waters, J. A., Königshof, P., Suttner, T. J., and Kido, E. (2019). Paleogeography and paleoenvironments of the late devonian kellwasser event: A review of its sedimentological and geochemical expression. *Glob. Planet. Change* 183, 102984. doi:10.1016/j.gloplacha.2019.102984

Carroll, A. R., Graham, S. A., Hendrix, M. S., Ying, D., and Zhou, D. (1995). Late Paleozoic tectonic amalgamation of northwestern China: Sedimentary record of the northern Tarim, northwestern Turpan, and southern Junggar Basins. *Geol. Soc. Am. Bull.* 107, 571–594. doi:10.1130/0016-7606(1995)107<0571:lptaon>2.3.co;2

Charvet, J., Shu, L., Laurent-Charvet, S., Wang, B., Faure, M., Cluzel, D., et al. (2011). Palaeozoic tectonic evolution of the Tianshan belt, NW China. *Sci. China Earth Sci.* 54, 166–184. doi:10.1007/s11430-010-4138-1

Chen, H., Yang, S., Wang, Q., Luo, J., Jia, C., Wei, G., et al. (2006). Sedimentary response to the Early-Mid Permian basaltic magmatism in the Tarim plate. *Geol. China* 33 (3), 545–552. doi:10.3969/j.issn.1000-3657.2006.03.010

Chen, R. (2000). On forming conditions for non-anticlinal oil and gas pools in the Tarim Basin. *Exp. Pet. Geol.* 22 (3), 215–219. doi:10.11781/sysydz200003215

Chen, S., Zhao, Z., Ji, W., Li, R., Liu, R., and Cha, X. (2013a). The characteristic of tectonic-lithofacies paleogeography during Early-Middle Permian in the west Kunlun and adjacent areas. *Chin. J. Geol.* 48 (4), 1015–1032. doi:10.3969/j.issn.0563-5020.2013.04.005

Chen, X., Dong, Y., Chen, H., and Wang, J. (2013b). Sequence structures and evolution patterns of the triassic in the platform of Tarim Basin. *Geol. Sci. Technol. Inf.* 32 (4), 50–54.

Clarke, J. W. (1984). Geology and possible uranium deposits of the Fergana region of soviet central Asia. *U. S. Geol. Surv.* doi:10.3133/ofr84513

Cocks, L. R. M., and Torsvik, T. H. (2013). The dynamic evolution of the Palaeozoic geography of eastern Asia. *Earth-Science Rev.* 117, 40–79. doi:10.1016/j.earscirev.2012.12.001

Dahlstrom, C. D. A. (1969). Balanced cross section. *Can. J. Geosciences* 6, 743–757. doi:10.1139/e69-069

Deledaer, C. (1996). Sedimentary system of carboniferous-permian of Western Tarim. *Xinjiang Geol.* 14 (4), 386–393. [in Chinese with English abstact.].

Dong, Y., He, D., Sun, S., Liu, X., Zhou, X., Zhang, F., et al. (2018). Subduction and accretionary tectonics of the East Kunlun Orogen, Western segment of the central China orogenic system. *Earth-Science Rev.* 186, 231–261. doi:10.1016/j.earscirev.2017.12.006

Dong, Y. P., Sun, S. S., Santosh, M., Zhao, J., Sun, J. P., He, D. F., et al. (2021). Central China orogenic belt and amalgamation of east asian continents. *Gondwana Res.* 100, 131–194. doi:10.1016/j.gr.2021.03.006

Eizenhöfer, P. R., Zhao, G. C., Sun, M., Zhang, J., Han, Y. G., and Hou, W. Z. (2015a). Geochronological and Hf isotopic variability of detrital zircons in Paleozoic strata across the accretionary collision zone between the North China craton and Mongolian arcs and tectonic implications. *GSA Bull.* 127, 1422–1436. doi:10.1130/B31175.1

Eizenhöfer, P. R., Zhao, G. C., Zhang, J., Han, Y. G., Hou, W. Z., Liu, D. X., et al. (2015b). Geochemical characteristics of the Permian basins and their provenances across the Solonker Suture Zone: Assessment of net crustal growth during the closure of the Palaeo-Asian Ocean. *Lithos* 224-225, 240–255.

Eizenhöfer, P. R., Zhao, G. C., Zhang, J., and Sun, M. (2014). Final closure of the paleo-Asian ocean along the solonker suture zone: Constraints from geochronological and geochemical data of permian volcanic and sedimentary rocks. *Tectonics* 33, 441–463. doi:10.1002/2013TC003357

Feng, Z., Peng, Y., Jin, Z., and Xiaozhang, S. (2004). *Lithofacies paleogeography of the cambrian and ordovician in China*. Beijing: Petroleum Industry Press.

Gao, H., He, D., Tong, X., Wen, Z., and Wang, Z. (2017). Tectonic-depositional environment and proto-type basin evolution of the cambrian in the Tarim Basin. *Geoscience* 31 (1), 102–118. doi:10.3969/j.issn.1000-8527.2017.01.009

Gao, J., Long, L., Klemd, R., Qian, Q., Liu, D., Xiong, X., et al. (2009). Tectonic evolution of the South tianshan orogen and adjacent regions, NW China: Geochemical and age constraints of granitoid rocks. *Int. J. Earth Sci.* 98, 1221–1238. doi:10.1007/s00531-008-0370-8

Gao, J., Zhu, M., and Wang, X. (2019). Large-scale porphyry-type mineralization in the central asian metallogenic domain: Tectonic background, fluid feature and metallogenic deep dynamic mechanism. *Acta Geol. Sin.* 93 (1), 24–71. doi:10.1016/j.jseaes.2017.10.002

Gao, R., Hou, H., Cai, X., Knapp, J., He, R., Liu, J., et al. (2013). Fine crustal structure beneath the junction of the southwest Tian Shan and Tarim Basin, NW China. *Lithosphere* 5 (4), 382–392. doi:10.1130/l248.1

Ge, R., Zhu, W., Wu, H., Zheng, B., Zhu, X., and He, J. (2012). The paleozoic northern margin of the Tarim craton: Passive or active? *Lithos* 142-143, 1–15. doi:10.1016/j.lithos.2012.02.010

Golonka, J., Krobicki, M., Pająk, J., Van Giang, N., and Zuchiewicz, W. (2006). "Global plate tectonics and paleogeography of Southeast Asia," in *Faculty of Geology, geophysics and environmental protection* (Arkadia, Kraków: AGH University of Science and Technology).

Gong, W. (2010). The deformational characteristics of the Tekilik thrust-nappe structures in southwest Tarim basin. *J. Oil Gas Technol.* 32 (5), 46–48. doi:10.3969/j.issn.1000-9752.2010.05.010

Görz, I., and Hielscher, P. (2010). An explicit plate kinematic model for the orogeny in the southern Uralides. *Tectonophysics* 493, 1–26. doi:10.1016/j.tecto.2010.07.005

Gu, J., Zhu, X., and Jia, J. (2003). *The deposits and reservoirs in the Tarim Basin*. Beijing: Petroleum Industry Press.

Guo, C., Gao, J., and Li, Z. (2018). Depositional and provenance records of lower Permian sandstones from Sishichang area, northwestern Tarim Basin: Implications for tectonic evolution. *Earth Sci.* 43 (11), 4149–4168.

Guo, R., Qin, Q., Muhetaer, Z., Zhao, L., Sun, M., and Wei, Z. (2013). Geological characteristics and tectonic significance of Ordovician granite intrusions in the Western segment of Quruqtagh, Xinjiang. *Earth Sci. Front.* 20 (4), 251–263.

Han, B. F., He, G. Q., Wang, X. C., and Guo, Z. J. (2011). Late carboniferous collision between the Tarim and Kazakhstan-Yili terranes in the Western segment of the South tian Shan orogen, central Asia, and implications for the northern Xinjiang, Western China. *Earth Sci. Rev.* 109 (3-4), 74–93. doi:10.1016/j.earscirev.2011.09.001

Han, B. F., Ji, J. Q., Song, B., Chen, L. H., and Zhang, L. (2006). Late Paleozoic vertical growth of continental crust around the Junggar Basin, Xinjiang, China (part I): Timing of post-collisional plutonism. *Acta Petrol. Sin.* 22 (5), 1077–1086. doi:10.3321/j.issn:1000-0569.2006.05.003

Han, Y., and Zhao, G. (2018). Final amalgamation of the tianshan and junggar orogenic collage in the southwestern central asian orogenic belt: Constraints on the closure of the paleo-Asian ocean. *Earth-Sci. Rev.* 186, 129–152. doi:10.1016/j.earscirev.2017.09.012

He, B., Jiao, C., Xu, Z., Cai, Z., Liu, S., Zhang, J., et al. (2015). Distribution and migration of the phanerozoic palaeo-uplifts in the Tarim Basin, NW China. *Earth Sci. Front.* 22 (3), 277–289. doi:10.13745/j.esf.2015.03.024

He, B., Jiao, C., Xu, Z., Cai, Z., Liu, S., and Zhang, Y. (2011). Manifestation of the middle-late caledonian tectonic movement along the altun-West Kunlun orogenic belt in the tangguzibas depression, Tarim basin. *Acta Petrol. Sin.* 27 (11), 3435–3448.

He, B., Jiao, C., Xu, Z., Cai, Z., and Yu, Z. (2016). The paleotectonic and paleogeography reconstructions of the Tarim Basin and its adjacent areas (NW China) during the late Early and Middle Paleozoic. *Gondwana Res.* 30, 191–206. doi:10.1016/j.gr.2015.09.011

He, D. F., Jia, C. Z., and Li, D. S. (2005). Formation and evolution of polycyclic superimposed Tarim Basin. *Oil Gas Geol.* 26 (1), 64–77. doi:10.11743/ogg20050109

He, D., Li, D., He, J., and Wu, X. (2013). Comparison in petroleum geology between Kuqa depression and Southwest depression in Tarim Basin and its exploration significance. *Acta Pet. Sin.* 34 (02), 201–218. doi:10.7623/syxb201302001

He, D., Li, D., Wang, C., Liu, S., and Chen, J. (2020). Status, thinking, and methodology of studying on the mobile tectono-palaeogeography. *J. Palaeogeogr. Chin. Ed.* 22 (1), 1–28. doi:10.7605/gdlxb.2020.01.001

He, D. (2022). Multi-cycle superimposed sedimentary basins in China: Formation, evolution, geologic framework and hydrocarbon occurrence. *Earth Sci. Front.* 29 (6), 024–059. doi:10.13745/j.esf.sf.2022.8.1

He, D., Zhou, X., Zhang, Z., and Yang, X. (2007). Types of Ordovician prototype basins in the Tarim region and their evolution. *Sci. Bull.* 52 (S1), 126–134. doi:10.1007/s11434-007-6010-z

He, Z. L., Gou, H. W., Li, X. R., and Yan, X. G. (1992). Prototype basin and sedimentary model of permo-carboniferous in Tarim plate. *Oil Gas Geol.* 13 (1), 1–14.

Hofmann, R., Goudemand, N., Wasmer, M., Bucher, H., and Hautmann, M. (2011). New trace fossil evidence for an early recovery signal in the aftermath of the end-Permian mass extinction. *Palaeogeogr. Palaeoclimatol. Palaeoecol.* 310, 216–226. doi:10.1016/j.palaeo.2011.07.014

Hou, F., Zhang, X., Wen, Z., Gao, Z., Feng, Y., Sun, J., et al. (2014). Paleogeographic reconstruction and tectonic evolution of major blocks in China since Paleozoic. *Mar. Geol. Quat. Geol.* 34 (6), 9–26. doi:10.3724/SP.J.1140.2014.06009

Hou, M. C., Chen, A. Q., Ogg, J. G., Ogg, G. M., Huang, K. K., Xing, F. C., et al. (2019). China paleogeography: Current status and future challenges. *Earth Sci. Rev.* 189, 177–193. doi:10.1016/j.earscirev.2018.04.004

Hu, X. M., Ma, A. L., Xue, W. W., Garzanti, E., Cao, Y., Li, S. M., et al. (2022). Exploring a lost Ocean in the Tibetan plateau: Birth, growth, and demise of the bangong-nujiang ocean. *Earth Sci. Rev.* 229, 104031. doi:10.1016/j.earscirev.2022.104031

Hu, Y., Zhang, Z., and Wang, E. (2010). Characteristics of different types of slope belt and its oil-control effect in Tarim Basin. *Lithol. Reserv.* 22 (4), 72–79. doi:10.3969/j.issn.1673-8926.2010.04.013

Huang, B. C., Yan, Y. G., Piper, J. D. A., Zhang, D. H., Yi, Z. Y., Yu, S., et al. (2018). Paleomagnetic constraints on the paleogeography of the East Asian blocks during late Paleozoic and early Mesozoic times. *Earth-Sci. Rev.* 186, 8–36. doi:10.1016/j.earscirev.2018.02.004

Huang, B., Zhou, Y., and Zhu, R. (2008). Discussions on Phanerozoic evolution and formation of continental China, based on paleomagnetic studies. *Earth Sci. Front.* 15 (3), 348–359. doi:10.3321/j.issn:1005-2321.2008.03.031

Huang, H., Wang, T., Tong, Y., Qin, Q., Ma, X., and Yin, J. (2020). Rejuvenation of ancient micro-continents during accretionary orogenesis: Insights from the Yili block and adjacent regions of the SW central asian orogenic belt. *Earth-Sci. Rev.* 208, 103255. doi:10.1016/j.earscirev.2020.103255

Huang, H. Y. (1986). Tectonic cycle characteristics in Xinjiang. *Northwest. Geol.* 1986, 10–18.

Huang, S., Xie, H., and Hou, G. (2023). The key transition of Chinese plates configuration in the early Paleoproterozoic. *J. Earth Sci.* In press.

Ingersoll, R. V. (2019). "Subduction-related sedimentary basins of the US cordillera," in *The sedimentary basins of the United States and Canada*. Editor A. D. Miall (Amsterdam, Netherlands: Elsevier), 477–510. doi:10.1016/B978-0-444-63895-3.00011-5

Ingersoll, R. V. (2012). "Tectonics of sedimentary basins, with revised nomenclature," in *Tectonics of sedimentary basins: Recent advances*. Editors B. Cathy (Antonio (Oxford, UK: Blackwell Publishing Ltd.), 1–43.

Jia, C., Wei, G., and Wang, L. (1997). *The structural characteristics and hydrocarbon of the Tarim Basin in China*. Beijing: Petroleum Industry Press.

Jia, C. Z., Sun, L. D., Zhou, X. Y., Gu, J. Y., Liang, D. G., Zhang, W., et al. (2004). *plate tectonics and continental dynamics in the Tarim Basin*. Beijing: Petroleum Industry Press.

Jia, D., Tian, J., Zhang, X., Zhu, H., Lin, X., Su, B., et al. (2017). Sequence stratigraphy and sedimentary evolution of donghe sandstone in Tarim Basin. *Oil Gas Geol.* 38 (6), 1123–1134. doi:10.11743/ogg20170613

Jiang, Z., Jiang, S., Lan, X., Wang, B., Huang, S., and Zhang, H. (2018). Neotectonic evolution of the Tarim Basin craton from neogene to quaternary. *Int. Geol. Rev.* 60 (10), 1213–1230. doi:10.1080/00206814.2017.1379365

Jolivet, M. (2015). Mesozoic tectonic and topographic evolution of central Asia and tibet: A preliminary synthesis. *Geol. Soc. Lond. Spec. Publ.* 427 (1), 19–55. doi:10.1144/sp427.2

Ju, Q., Zhang, Y. C., Yuan, D. X., Qiao, F., Xu, H. P., Zhang, H., et al. (2022). Permian foraminifers from the exotic limestone blocks within the central Qiangtang Metamorphic Belt, Tibet and their geological implications. *J. Asian Earth Sci.* 239, 105426. doi:10.1016/j.jseaes.2022.105426

Korobkin, V. V., and Buslov, M. M. (2011). Tectonics and geodynamics of the Western central Asian fold belt (Kazakhstan paleozoides). *Russ. Geol. Geophys.* 52, 1600–1618. doi:10.1016/j.rgg.2011.11.011

Laborde, A., Barrier, L., Simoes, M., Li, H., Coudroy, T., Van der Woerd, J., et al. (2019). Cenozoic deformation of the Tarim Basin and surrounding ranges (Xinjiang, China): A regional overview. *Earth-Sci. Rev.* 197, 102891. doi:10.1016/j.earscirev.2019.102891

Li, H., Wang, J., Wu, G., Shi, L., Wang, B., Hu, X., et al. (2014c). Features and formation mechanism of middle Caledonian faults in west of Tangguzibasi depression, Tarim Basin. *J. Central South Univ. Sci. Technol.* 45 (12), 4331–4341.

Li, J., and Jiang, H. (2013). *World atlas of Plate Tectonic reconstruction, lithofacies paleogeography and plaeoenvironment*. Beijing: Geological Publishing House.

Li, J., Wang, H., Li, W., and Zhou, X. (2014a). Discussion on global tectonics evolution from plate reconstruction in Phanerozoic. *Acta Pet. Sin.* 35 (2), 207–218. doi:10.7623/syxb201402001

Li, J., Zhou, X., Li, W., Wang, H., Liu, Z., Zhang, H., et al. (2015). Preliminary reconstruction of tectonic paleogeography of Tarim Basin and its adjacent aeras from cambrian to triassic, NW China. *Geol. Rev.* 61 (6), 1225–1234.

Li, S., Zhao, S., Liu, X., Cao, H., Yu, S., Li, X., et al. (2018). Closure of the proto-tethys Ocean and early paleozoic amalgamation of microcontinental blocks in east Asia. *Earth-Science Rev.* 186, 37–75. doi:10.1016/j.earscirev.2017.01.011

Li, S. Z., Kang, Z. H., and Meng, M. M. (2014b). Permian sedimentary environment evolution in southwest Tarim. *Xinjiang Geol.* 32 (4), 451–456. doi:10.3969/j.issn.1000-8845.2014.04.005

Li, W., Zhang, Z., and Lin, T. (2021). Analysis of the boundary properties of the Tarim block during the main tectonic period. *Chem. Eng. Des. Commun.* 47 (10), 11–12. doi:10.3969/j.issn.1003-6490.2021.10.006

Li, Y., Robinson, A. C., Gadoev, M., and Oimuhammadzoda, I. (2020). Was the Pamir salient built along a late paleozoic embayment on the southern asian margin? *Earth Planet. Sci. Lett.* 550, 116554. doi:10.1016/j.epsl.2020.116554

Li, Z., Gao, J., Guo, C., and Xu, J. (2015). Devonian-Carboniferous tectonic evolution of continental margins in northern Tarim block, Northwest China: Constrained by basin-fill sequences and provenance system. *Earth Sci. Froniters* 2015, 35–52. [in Chinese with English abstract].

Lin, B., Zhang, X., Xu, X., Yuan, J., Neng, Y., and Zhu, J. (2015). Features and effects of basement faults on deposition in the Tarim Basin. *Earth-Sci. Rev.* 145, 43–55. doi:10.1016/j.earscirev.2015.02.008

Lin, C., Li, S., Liu, J., Qian, Y., Luo, H., Chen, J., et al. (2011). Tectonic framework and paleogeographic evolution of the Tarim basin during the Paleozoic major evolutionary stages. *Acta Petrol. Sin.* 27 (1), 210–218.

Lin, C. S., Yang, H. J., Liu, J. Y., Rui, Z. F., Cai, Z. Z., Li, S. T., et al. (2012a). Sequence architecture and depositional evolution of the Ordovician carbonate platform margins in the Tarim Basin and its response to tectonism and sea-level change. *Basin Res.* 24 (5), 559–582. doi:10.1111/j.1365-2117.2011.00536.x

Lin, C. S., Yang, H. J., Liu, J. Y., Rui, Z. F., Cai, Z. Z., and Zhu, Y. F. (2012b). Distribution and erosion of the Paleozoic tectonic unconformities in the Tarim Basin, Northwest China: Significance for the evolution of paleo-uplifts and tectonic geography during deformation. *J. Asian Earth Sci.* 46, 1–19. doi:10.1016/j.jseaes.2011.10.004

Lin, C., Yang, H., Liu, J., Peng, L., Cai, Z., Yang, X., et al. (2009). Paleostructural geomorphology of the Paleozoic central uplift belt and its constraint on the development of depositional facies in the Tarim Basin. *Sci. China Ser. D Earth Sci.* 52 (6), 823–834. doi:10.1007/s11430-009-0061-8

Liu, D., Guo, Z., Jolivet, M., Cheng, F., Song, Y., and Zhang, Z. (2014a). Petrology and geochemistry of early permian volcanic rocks in south tian Shan, NW China: Implications for the tectonic evolution and phanerozoic continental growth. *Int. J. Earth Sci.* 103 (3), 737–756. doi:10.1007/s00531-013-0994-1

Liu, H., Somerville, I., Lin, C., and Zuo, S. (2016). Distribution of palaeozoic tectonic superimposed unconformities in the Tarim Basin, NW China: Significance for the evolution of palaeogeomorphology and sedimentary response. *Geol. J.* 51, 627–651. doi:10.1002/gj.2664

Liu, J. D., Qi, L. X., Tian, J. C., Li, Z. J., and Zhang, X. B. (2014b). *Tectonic evolution and sedimentary lattice in the Tarim Basin*. Beijing: Science Press.

Liu, J., Lin, C., Peng, L., Chen, Q., Zhang, X., and Zhou, X. (2008). Distribution patterns of the end of the Middle Devonian tectonic unconformity and their constrain on the development and distribution of favorable stratigraphic traps in the Tarim Basin. *Oil Gas Geol.* 29 (2), 268–275. doi:10.11743/ogg20080217

Liu, K., Wang, Y., Jiang, G., Zhang, S., and Zhang, K. (2014c). Evolution of Neoproterozoic-Mesozoic sedimentary basins of west Kunlun area. *Earth Science-Journal China Univ. Geosciences* 39 (8), 987–999. doi:10.3799/dqkx.2014.090

Liu, X., Graham, S., Chang, E., Wu, S., Fu, D., Yao, J., et al. (1994). Tectonic evolution of Tarim plate and its surrounding area since Late Paleozoic. *Earth Science-Journal China Univ. Geosciences* 19 (6), 715–725.

Liu, X., Zhang, X., Liu, L., Li, B., Zhang, X., Song, H., et al. (2014d). The new achievements and main progress in regional geological exploration and mineral resources survey of Karaqi area, Xinjiang. *Geol. Bull. China* 33 (1), 1–8. doi:10.3969/j.issn.1671-2552.2014.01.002

Liu, Y., Li, W., Feng, Z., Wen, Q., Neubauer, F., and Liang, C. (2017). A review of the paleozoic tectonics in the eastern part of central asian orogenic belt. *Gondwana Res.* 43, 123–148. doi:10.1016/j.gr.2016.03.013

Lou, Q. Q., Xiao, A. C., Zhong, N. C., and Wu, L. (2016). A method of proto-type restoration of large depressions with terrestrial sediments: A case study from the cenozoic Qaidam basin. *Acta Petrol. Sin.* 32 (03), 892–902. (in Chinese).

Luo, J., Che, Z., Zhang, G., Nian, X., and Zhang, X. (2012). Early-Middle Permian basin-mountain coupling features between northwestern margin of the Tarim basin and the South Tianshan orogen. *Acta Petrol. Sin.* 28 (8), 2506–2514.

Ma, C., Li, J., Cao, Z., Liu, L., and Wang, M. (2020). Lithofacies paleogeographic reconstruction and evolution of the Carboniferous-Permian basin group in Central Asia. *Acta Petrol. Sin.* 36 (11), 3510–3522. doi:10.18654/1000-0569/2020.11.16

Ma, Q., Ma, T., Yang, H., Zhao, X., and Zhu, Y. (2019). Development characteristics of the third-order sequence of upper devonian-lower carboniferous shore-mixed shelf in Tarim Basin, NW China. *Petroleum Explor. Dev.* 46 (04), 701–710. doi:10.1016/s1876-3804(19)60227-2

Ma, X., Shu, L., Meert, J., and Li, J. (2014). The paleozoic evolution of central tianshan: Geochemical and geochronological evidence. *Gondwana Res.* 25 (2), 797–819. doi:10.1016/j.gr.2013.05.015

Matte, Ph., Tapponnier, P., Arnaud, N., Bourjot, L., Avouac, J. P., Vidal, Ph., et al. (1996). Tectonics of western tibet, between the Tarim and the indus. *Earth Planet. Sci. Lett.* 142, 311–330. doi:10.1016/0012-821x(96)00086-6

Moisan, P., Voigt, S., Pott, C., Buchwitz, M., Schneider, J. W., and Kerp, H. (2011). Cycadalean and bennettitalean foliage from the triassic madygen lagerstätte (SW Kyrgyzstan, central Asia). *Rev. Palaeobot. Palynol.* 164 (1-2), 93–108. doi:10.1016/j.revpalbo.2010.11.008

Müller, R. D., Cannon, J., Qin, X., Watson, R. J., Gurnis, M., Williams, S., et al. (2018). GPlates: Building a virtual Earth through deep time. *Geochem. Geophys. Geosystems* 19, 2243–2261. doi:10.1029/2018GC007584

Niu, Y. Z., Shi, G. R., Ji, W. H., Zhou, J. L., Wang, J. Q., Wang, K., et al. (2021). Paleogeographic evolution of a Carboniferous-Permian sea in the southernmost part of the Central Asian Orogenic Belt, NW China: Evidence from microfacies, provenance and paleobiogeography. *Earth-Science Rev.* 220, 103738. doi:10.1016/j.earscirev.2021.103738

Pan, G., Li, X., Wang, L., Ding, J., and Chen, Z. (2002). Preliminary division of tectonic units of the Qinghai-Tibet Plateau and its adjacent regions. *Geol. Bull. China* 21 (11), 701–707. doi:10.3969/j.issn.1671-2552.2002.11.002

Pu, R., Yun, L., Su, J., Guo, Q., and Dang, X. (2014). Growth conditions and 3-D seismic delineation of carboniferous barrier reefs in the southwestern Tarim Basin. *J. Earth Sci.* 2014, 315–323. doi:10.1007/s12583-014-0429-3

Pullen, A., Kapp, P., Gehrels, G. E., Vervoort, J. D., and Ding, L. (2008). Triassic continental subduction in central tibet and mediterranean-style closure of the Paleo-Tethys Ocean. *Geology* 36 (5), 351–354. doi:10.1130/g24435a.1

Qi, L., Li, Z., and Lü, H. (2020). *Tectonic sedimentary evolution and oil and gas exploration in Tarim superimposed basin*. Beijing: Science Press.

Ren, R., Guan, S. W., Han, B. F., and Su, L. (2017). Chronological constraints on the tectonic evolution of the Chinese Tianshan Orogen through detrital zircons from modern and palaeo-river sands. *Int. Geol. Rev.* 59, 1657–1676. doi:10.1080/00206814.2017.1292468

Robinson, A. C., Yin, A., Manning, C. E., Harrison, T. M., Zhang, S.-H., and Wang, X.-F. (2007). Cenozoic evolution of the eastern Pamir: Implications for strain-accommodation mechanisms at the Western end of the Himalayan-Tibetan Orogen. *Geol. Soc. Am. Bull.* 119 (7/8), 882–896. doi:10.1130/b25981.1

Schwab, M., Ratschbacher, L., Siebel, W., McWilliams, M., Minaev, V., Lutkov, V., et al. (2004). Assembly of the Pamirs: Age and origin of magmatic belts from the southern Tien Shan to the southern Pamirs and their relation to Tibet. *Tectonics* 23, TC4002. doi:10.1029/2003tc001583

Sobel, E., and Dumitru, T. (1997). Thrusting and exhumation around the margins of the Western Tarim basin during the India-Asia collision. *J. Geophys. Res. Solid Earth* 102, 5043–5063. doi:10.1029/96jb03267

Song, P. P., Ding, L., Li, Z. Y., Lippert, P., Yang, T. S., Zhao, X. X., et al. (2015). Late triassic paleolatitude of the Qiangtang block: Implications for the closure of the Paleo-Tethys Ocean. *Earth Planet. Sci. Lett.* 424, 69–83. doi:10.1016/j.epsl.2015.05.020

Su, B. R. (2019). *Sedimentary records, provenance analysis and paleogeography of the Donghetang Formation of late devonian in Tarim basin* ([Chengdu (Sichuan)]: Chengdu University of Technology). [dissertation/Doctoral thesis].

Su, W., Gao, J., Klemd, R., Li, J., Zhang, X., Li, X., et al. (2010). U-Pb zircon geochronology of tianshan eclogites in NW China: Implication for the collision between the Yili and Tarim blocks of the southwestern altaids. *Eur. J. Mineralogy* 22 (4), 473–478. doi:10.1127/0935-1221/2010/0022-2040

Tapponnier, P., Xu, Z., Roger, F., Mayer, B., Arnaud, N., Wittlinger, G., et al. (2001). Oblique stepwise rise and growth of the Tibet plateau. *Science* 294, 1671–1677. doi:10.1126/science.105978

Van der Voo, R., Levashova, N. M., Skrinnik, L. I., Kara, T. V., and Bazhenov, M. L. (2006). Late orogenic, large-scale rotations in the Tien Shan and adjacent mobile belts in Kyrgyzstan and Kazakhstan. *Tectonophysics* 426, 335–360. doi:10.1016/j.tecto.2006.08.008

Wan, T., and Zhu, H. (2007). Positions and kinematics of Chinese continental blocks in reconstruction of global paleo-continents for Paleozoic and Triassic. *Geoscience* 21 (1), 1–13. doi:10.3969/j.issn.1000-8527.2007.01.001

Wang, B., Chen, Y., Zhan, S., Shu, L. S., Faure, M., Cluzel, D., et al. (2007). Primary carboniferous and permian paleomagnetic results from the Yili block (NW China) and their implications on the geodynamic evolution of Chinese tianshan belt. *Earth Planet. Sci. Lett.* 263, 288–308. doi:10.1016/j.epsl.2007.08.037

Wang, C., Tang, H., Zheng, Y., Dong, L., Li, J., and Qu, X. (2019). Early Paleozoic magmatism and metallogeny related to Proto-Tethys subduction: Insights from volcanic rocks in the northeastern Altyn Mountains, NW China. *Gondwana Res.* 75, 134–153. doi:10.1016/j.gr.2019.04.009

Wang, Q., Li, S., Zhao, S., Mu, D., Guo, R., and Somerville, I. (2017). Early paleozoic Tarim orocline: Insights from paleogeography and tectonic evolution in the Tarim Basin. *Geol. J.* 52 (S1), 436–448. doi:10.1002/gj.2985

Wang, T., Jin, Z., Li, H., et al. (2020a). Processes and causes of Phanerozoic tectonic evolution of the Western Tarim Basin, northwest China. *Pet. Sci.* 17, 279–291. doi:10.1007/s12182-019-00424-x

Wang, T., Jin, Z., Shi, Z., Dai, X., and Cheng, R. (2020b). Phanerozoic plate history and structural evolution of the Tarim Basin, northwestern China. *Int. Geol. Rev.* 62 (12), 1555–1569. doi:10.1080/00206814.2019.1661038

Wang, X., Klemd, R., Li, J., Gao, J., Jiang, T., Zong, K., et al. (2022). Paleozoic subduction-accretion in the southern central asian orogenic belt: Insights from the wuwamen accretionary complex of the Chinese South Tianshan. *Tectonics* 41, e2021TC006965. doi:10.1029/2021tc006965

Wilhem, C., Windley, B. F., and Stampfli, G. M. (2012). The altaids of central Asia: A tectonic and evolutionary innovative review. *Earth Sci. Rev.* 113, 303–341. doi:10.1016/j.earscirev.2012.04.001

Windley, B. F., Alexeiev, D., Xiao, W., Kröner, A., and Badarch, G. (2007). Tectonic models for accretion of the central asian orogenic belt. *J. Geol. Soc.* 164, 31–47. doi:10.1144/0016-76492006-022

Windley, B. F., Allen, M. B., Zhang, C., Zhao, Z. Y., and Wang, G. R. (1990). Paleozoic accretion and cenozoic redeformation of the Chinese tien Shan range, central Asia. *Geology* 18 (2), 128. doi:10.1130/0091-7613(1990)018<0128:paacro>2.3.co;2

Woodcock, N. H. (2004). Life span and fate of basins. *Geology* 32, 685–688. doi:10.1130/g20598.1

Wu, G., Deng, W., Huang, S., Zheng, D., and Pan, W. (2020). Tectonic-paleogeographic evolution in the Tarim Basin. *Chin. J. Geol.* 55 (2), 305–321. doi:10.12017/dzkx.2020.020

Wu, G., Li, Y., Liu, Y., and Zhao, Y. (2013). Paleozoic sediment-tectonic evolution and basin dynamic settings in Wushi-Kalpin-Bachu area, northwest Tarim. *J. Palaeogeogr.* 15 (2), 203–218. doi:10.7605/gdlxb.2013.02.018

Wu, G., Pang, X., and Li, M. (2016). *The structural characteristics of carbonate rocks and their effects on hydrocarbon exploration in craton basin: A case study of the Tarim Basin*. Beijing: Science Press.

Xiao, W., Han, C., Yuan, C., Sun, M., Lin, S., Chen, H., et al. (2008). Middle cambrian to permian subduction-related accretionary orogenesis of northern Xinjiang, NW China: Implications for the tectonic evolution of central Asia. *J. Asian Earth Sci.* 32, 102–117. doi:10.1016/j.jseaes.2007.10.008

Xiao, W. J., Windley, B. F., Allen, M., and Han, C. M. (2013). Paleozoic multiple accretionary and collisional tectonics of the Chinese Tianshan orogenic collage. *Gondwana Res.* 23, 1316–1341. doi:10.1016/j.gr.2012.01.012

Xiao, W. J., Windley, B. F., Yuan, C., Sun, M., Han, C. M., Lin, S. F., et al. (2009). Paleozoic multiple subduction-accretion processes of the southern Altaids. *Am. J. Sci.* 309, 221–270. doi:10.2475/03.2009.02

Xiao, W., and Santosh, M. (2014). Paleozoic multiple accretionary and collisional tectonics of the Chinese Tianshan orogenic collage. *Gondwana Res.* 25, 1429–1444. doi:10.1016/j.gr.2014.01.008

Xiao, W., Zhou, H., Windley, B. F., Yuan, C., Chen, H., Zhang, G., et al. (2003). Structures and evolution of the multiple accretionary complexes, western Kunlun orogenic belt (China). *Xinjiang Geol.* 21 (1), 31–36.

Xie, X., Wu, Q., and Lu, H. (1997). Tectonic framework and sedimentary feature of the Tarim Basin in paleozoic. *Acta Sedimentol. Sin.* 15 (1), 153–156.

Xu, J. (2009). *Sequence stratigraphy of upper devonian-carboniferous in Tarim Basin* ([Changsha (Hunan)]: Central South University). [dissertation/Doctoral thesis].

Xu, Z., Dilek, Y., Cao, H., Yang, J., Robinson, P., Ma, C., et al. (2015). Paleo-tethyan evolution of tibet as recorded in the east cimmerides and west cathaysides. *J. Asian Earth Sci.* 105, 320–337. doi:10.1016/j.jseaes.2015.01.021

Xu, Z., Li, S., Zhang, J., Yang, J., He, B., Li, H., et al. (2011). Paleo-Asian and Tethyan tectonic systems with docking the Tarim block. *Acta Petrol. Sin.* 27 (1), 1–22.

Yan, M., Zhang, D., Fang, X., Ren, H., Zhang, W., Zan, J., et al. (2016). Paleomagnetic data bearing on the mesozoic deformation of the Qiangtang block: Implications for the evolution of the paleo- and meso-tethys. *Gondwana Res.* 39, 292–316. doi:10.1016/j.gr.2016.01.012

Yang, D., Li, S., Wang, S., Wan, Q., Zhao, D., and Xu, J. (2011). Detrital composition of Upper Carboniferous sandstone in northern Tarim basin and its implications for provenance and tectonic attributes. *Acta Petrologica Mineralogica* 30 (4), 645–653. doi:10.3969/j.issn.1000-6524.2011.04.008

Ye, L., Wang, G., and Zhai, X. (1997). Geology of the Kuqa river and Kalpin, Tarim Basin. *Xinjing Geol.* 15 (2), 174–192.

Yi, Z. Y., Huang, B. C., Xiao, W. J., Yang, L. K., and Qiao, Q. Q. (2015). Paleomagnetic study of late paleozoic rocks in the tacheng basin of west junggar (NW China): Implications for the tectonic evolution of the Western altaids. *Gondwana Res.* 27, 862–877. doi:10.1016/j.gr.2013.11.006

Yu, H. B., Qi, J. F., Yang, X. Z., Sun, T., Liu, Q. X., and Cao, S. J. (2016). Analysis of mesozoic proto-type basin in kuga depression, Tarim Basin. *Xinjiang Pet. Geol.* 37 (06), 644–653+666. (in Chinese with English abstract). doi:10.7657/XJPG20160604

Zhang, B., Chen, W., Yu, S., Yin, J., Li, J., Sun, J., et al. (2014a). Subduction process of South Tianshan ocean during paleozoic. *Acta Petrol. Sin.* 30 (8), 2351–2362. (in Chinese with English abstract).

Zhang, C. L., Ye, X. T., Zou, H. B., and Chen, X. Y. (2016). Neoproterozoic sedimentary basin evolution in southwestern Tarim, NW China: New evidence from field observations, detrital zircon U-Pb ages and Hf isotope compositions. *Precambrian Res.* 280, 31–45. doi:10.1016/j.precamres.2016.04.011

Zhang, C. L., Zou, H. B., Ye, X. T., and Chen, X. Y. (2019a). Tectonic evolution of the West Kunlun orogenic belt along the northern margin of the Tibetan plateau: Implications for the assembly of the Tarim terrane to Gondwana. *Geosci. Front.* 10 (3), 973–988. doi:10.1016/j.gsf.2018.05.006

Zhang, C., Ma, H., and Liu, X. (2022). Architecture and tectonic evolution of the Pamir plateau: A review. *Geol. Rev.* 68 (5), 1653–1673.

Zhang, G., Liu, W., Zhang, L., Xu, B., Li, H. H., Zhang, B., et al. (2015). Cambrian-Ordovician prototypic basin, paleogeography and petroleum of Tarim Craton. *Earth Sci. Front.* 22 (3), 269–276. doi:10.13745/j.esf.2015.03.023

Zhang, G., Tong, X., Xin, R., Wen, Z., Ma, F., Huang, T., et al. (2019b). Evolution of lithofacies and paleogeography and hydrocarbon distribution worldwide (I). *Petroleum Explor. Dev.* 46, 664–686. doi:10.1016/s1876-3804(19)60225-9

Zhang, G., Zhao, W., Wang, H., Li, H., and Liu, L. (2007a). Multicycle tectonic evolution and composite petroleum systems in the Tarim Basin. *Oil Gas Geol.* 28 (5), 653–663. doi:10.11743/ogg20070517

Zhang, H., Yang, H., Shou, J., Zhang, R., Geng, Z., and Wang, B. (2009a). Sedimentary periods of Donghe sandstone and hydrocarbon exploration in Tarim Basin. *Acta Pet. Sin.* 30 (6), 835–842. doi:10.7623/syxb200906008

Zhang, J., Luo, J., Qing, Y., Cao, Y., and Fan, J. (2007b). The sedimentary feature and structure significance of turbidite Carboniferous Permian on the northwestern margin of the Tarim Basin. *J. Northwest Univ. Nat. Sci. Ed.* 37 (5), 819–824.

Zhang, L., Zhang, B., Dong, Z., Xie, Y., Li, W., Peng, Z., et al. (2020). Tectonic setting and metallogenetic conditions of Carboniferous Malkansu giant manganese belt in West Kunlun Orogen. *J. Jilin Univ. (Earth Sci. Ed.* 50 (5), 1340–1357. doi:10.13278/j.cnki.jjuese.20190294

Zhang, M., and Chen, F. (1998). Application condition of balanced-section technique and the case analysis. *Oil Geophys. Prospect.* 33 (4), 532–540.

Zhang, M., Wang, G. C., Zhang, X. H., Liao, Q. A., Wang, W., Guo, R. L., et al. (2021). Reconstruction of the silurian to devonian stratigraphic succession along the northeastern margin of the junggar block, Xinjiang, NW China, and its tectono-paleogeographic implications for the southwestern central asian orogenic belt. *Sediment. Geol.* 411, 105780. doi:10.1016/j.sedgeo.2020.105780

Zhang, X. B., Zhang, S. N., Zhao, X. K., He, J. J., Li, K., Dai, H. S., et al. (2007c). Calculation of denudation thickness of superimposed basin by seism stratigraphic comprehensive method: A case study from the akekule uplift in Tarim Basin. *Xinjiang Pet. Geol.* 2007, 366–368. (in Chinese). doi:10.3969/j.issn.1001-3873.2007.03.030

Zhang, X., Tian, J., and Peng, J. (2008). The lithofacies-paleogeography and space-time evolvement of Silurian-Devonian in the Tarim Basin. *Acta Sedimentol. Sin.* 26 (5), 762–771.

Zhang, Y., He, D., and Liu, C. (2019c). Three-dimensional geological structure and genetic mechanism of the Bachu uplift in the Tarim Basin. *Earth Sci. Front.* 26 (1), 134–148. doi:10.13745/j.esf.sf.2019.1.1

Zhang, Z., Wang, Y., Yun, J., Zhou, B., Zhao, Z., and Zheng, M. (2009b). Control of faults at different evolution stages on hydrocarbon accumulation in Tazhong area, the Tarim Basin. *Oil Gas Geol.* 30 (3), 316–323. doi:10.11743/ogg20090310

Zhao, G. C., Wang, Y. J., Huang, B. C., Dong, Y. P., Li, S. Z., Zhang, G. W., et al. (2018). Geological reconstructions of the east asian blocks: From the breakup of rodinia to the assembly of Pangea. *Earth Sci. Rev.* 186, 262–286. doi:10.1016/j.earscirev.2018.10.003

Zhao, J., Liu, G., Lu, Z., Zhang, X., and Zhao, G. (2003). Lithospheric structure and dynamic processes of the Tianshan orogenic belt and the Junggar basin. *Tectonophysics* 376, 199–239. doi:10.1016/j.tecto.2003.07.001

Zhao, X., Coe, R. S., Zhou, Y. X., Wu, H. R., and Wang, J. (1990). New palaeomagnetic results from northern China: Collision and suturing with Siberia and Kazakhstan. *Tectonophysics* 181, 43–81.

Zhao, Z., Luo, J., and Zhang, Y. (2011). Lithofacies paleogeography of cambrian sequences in the Tarim Basin. *Acta Pet. Sin.* 32 (6), 937–948.

Zhao, Z., Wu, X., Pan, W., Zhang, X., Zhang, L., Ma, P., et al. (2009). Sequence lithofacies and paleogeography of ordovician in Tarim Basin. *Acta Sedimentol. Sin.* 27 (5), 939–955. (in Chinese with English abstract).

Zheng, H., Tian, J., Hu, Z., Zhang, X., Zhao, Y., and Meng, W. (2022). Lithofacies palaeogeographic evolution and sedimentary model of the Ordovician in the Tarim Basin. *Oil Gas Geol.* 43 (4), 733–745. doi:10.11743/ogg20220401

Zhou, R. Q., Fu, H., Xu, G. S., and Gao, Y. F. (2014). The opening-closing of surrounding ocean Basin in response to tectonic-sedimentation in Tarim Basin. *Sci. Technol. Eng.* 14 (35), 1671–1815. doi:10.3969/j.issn.1671-1815.2014.35.002

Zhu, H., Su, B., Jia, D., and Li, C. (2016). Sedimentary facies plane distribution characteristics of central uplift belt in different periods in Donghetang Formation. *Coal Technol.* 35 (7), 105–107. doi:10.13301/j.cnki.ct.2016.07.043

Zhu, R., Xu, H., Deng, S., and Guo, H. (2007). Lithofacies palaeogeography of the Permian in northern China. *J. Palaeogeogr.* 9 (2), 133–142. doi:10.3969/j.issn.1671-1505.2007.02.002

Zhuang, X., Xiao, L., and Yang, J. (2002). Sedimentary facies in southwestern region of Tarim Basin. *Xinjiang Geol.* 20, 78–82. doi:10.3969/j.issn.1000-8845.2002.z1.014

Zou, Y., Ta, J., Xing, Z., Xu, Z., Tang, T., and Hao, Y. (2014). Evolution of sedimentary basins in Tarim during neoproterozoic-paleozoic. *Earth Science-Journal China Univ. Geosciences* 39 (8), 1200–1216.